Decreasing uplift rates and Pleistocene marine terraces settlement in the central lesser Antilles fore-arc (La Desirade Island, 16 degrees N)

Jean-Len Leticee, Jean-Jacques Cornee, Philippe Munch, Jan Fietzke, Melody Philippon, Jean-Frederic Lebrun, Lyvane de Min, Auran Randrianasolo

Decreasing uplift rates and Pleistocene marine terraces settlement in the central lesser Antilles fore-arc (La Désirade Island, 16°N)

Jean-Len Léticée, [a] Jean-Jacques Cornée, [a, b*], Philippe Münch [b], Jan Fietzke[c], Mélodie Philippon [a], Jean-Frédéric Lebrun [a], Lyvane De Min [a,b], Auran Randrianasolo [a]

[a] *Géosciences Montpellier, Université des Antilles, CNRS, Pointe à Pitre, Guadeloupe, FWI*

[b] *Géosciences Montpellier, Université de Montpellier, CNRS, Montpellier, France*

[c] *GEOMAR, Helmholtz Centre for Ocean Research, Kiel, Wischhofstr, 1-3, 24148 Kiel Germany*

Corresponding author: jean-jacques.cornee@gm.univ-montp2.fr (J.-J. Cornée)

Abstract

This study investigates the Lesser Antilles forearc at the latitude of Guadeloupe Archipelago and evidences that La Désirade Island, the eastermost island of the forearc, displays a staircase coastal sequence including four uplifted marine terraces and an upper reefal platform with mean shoreline angle elevations ranging from 10 and 210 m above sea level (asl). The platform paleobathymetry is constraint by a detailed analysis of the sediments. We propose a revised morphostratigraphy for this coastal sequence including 5 paleo-shorelines based on six U/Th dating from aragonitic corals from the three lowest terraces combined with paleobathymetric analysis of the fossil corals present in the upper platform allow. Terrace and upper platform carving of construction periods occurred during Marine Isotopic Stages MIS 5e, MIS 9, and during the intervals MIS 15-17, MIS 19-25 and MIS 31-49 (upper coral reef platform). Our results evidence a bulk decreasing uplift rate since early Calabrian to Present-Day, clearly documented since 310 ka (MIS 9) (from 0.14-0.19 to *ca* 0 mm/y). Our data are consistent with first the transient influence of the subducting oceanic Tiburon ridge during Calabrian, then with other parametres of the subduction zone since late Calabrian to Present-Day (dip of the slab, basal erosion of the upper plate, inherited structures…) .

Keywords: Pleistocene; Lesser Antilles subduction; La Désirade; coral reef terraces; uplift; Tiburon Ridge.

1. Introduction

Strain pattern and rates observed in fore-arcs of subduction zones are controlled by subduction dynamics, sediment supply at the trench and structural inheritances affecting the upper plate (Noda, 2016). In particular, vertical motions in fore-arcs can result from several mechanisms such as: (i) varying geodynamical subduction regime (compressional or extensional) (Shemenda, 1994; Lallemand, 1999), (ii) basal tectonic erosion of the upper plate or accretionary processes (von Huene and Culotta, 1989; Lallemand, 1995; Clift and Vanucci, 2004), (iii) subduction of downgoing plate asperities (such as seamounts, spreading ridges or fracture zone ridges) (e.g. Collot and Fisher,1989; Dominguez et al., 1998, 2000), (iv) or strain partitioning during oblique subduction driving positive or negative flower structures along strike-slip faults (Gutscher et al., 1998; von Huene et al., 2003; Barnes and Nicol, 2004). Thus, the study and quantification of the distribution and wavelenght of vertical tectonic motions through space and time is key to determine long-term subduction dynamics, but also to assess seismic hazards in subduction zones.

Submerged and/emerged sequences of marine terraces are very useful datable paleosea levels markers as they allow for calculating uplift or subsidence rates (e.g. Henry et al., 2014; Pedoja et al., 2011, 2014; Saillard et al., 2009, 2011). Coastal uplift rates since MIS 5e have been found significantly higher in highly coupled subduction zones than in other geodynamic settings (Pedoja et al., 2011; Henry et al., 2014). Moreover, coastal uplift rates in fore-arc settings have been found correlated mainly with the distance to the trench (with decreasing uplift rates landward up to ~300 km), the slab dip and the position along the trench (Henry et al., 2014). The tectonic regime of the subduction margin (erosive *vs* accretionary) and the overriding plate tectonic regime (compressive *vs* extensive) appear only gently correlated (Henry et al., 2014; Noda, 2016). Noticeably, the convergence velocity,

subduction obliquity, oceanic crust age, interplate friction force and overriding plate velocity do not appear correlated with coastal uplift rates of fore-arcs (Henry et al., 2014).

The Lesser Antilles subduction is considered as a weakly coupled accretionary subduction zone where an old oceanic lithosphere slowly subducted (2cm/an) beneath the Caribbean plate and with an accretionnary compressional fore-arc basin ((e.g. Von Huene and Scholl, 1991; Clift and Vannucchi, 2004; Noda, 2016). This description corresponds well to the southern Lesser Antilles where an uplifted sequence of marine terraces has been extensively studied in the outer fore-arc, in the Barbados Island (e.g. Taylor and Mann, 1991; Schellmann and Radtke, 2004). However many sequences of marine terraces also occur in the central Lesser Antilles fore-arc, i.e. to the North of the Martinique Island, but have been more scarcely studied (Désirade: Battistini et al., 1986; Marie-Galante : Feuillet et al., 2004). North of Martinique, the Lesser Antilles subduction zone has a different tectonic regime from the one at the latitude of the Barbados Island exemplified by a narrowed accretionnary prism, an extensional overriding plate tectonic regime (Feuillet et al., 2002; De min et al., 2014), the subduction of sediments deeper into the subduction zone (Bangs et al., 2003) and the subduction of aseismic ridges (Bouysse and Westercamp, 1988). We detail here the quantification of vertical motion in La Désirade Island, i.e. the easternmost island (185 km west of the trench) island of the fore-arc, since ~1.5 Ma. In La Désirade Island, a stair-cased marine terraces sequence has been identified since a long time (Lasserre, 1957; Battistini et al., 1986) and Pliocene–Pleistocene carbonate platform deposits reach 210 m in elevation (Andreïeff et al., 1989; Münch et al., 2013). To reach this goal, we acquired a new sedimentological, geomorphological and radiochronological dataset from uplifted constructed (corals) marine terraces and reefal carbonate platforms. This dataset allows us to calculate mean coastal uplift rates of the fore-arc since ~1.5 Ma and to discuss about the fore-arc tectonic structures responsible for terraces uplift and, at subduction-scale, the mechanical behavior of the subduction interface at 16°N latitude in the Caribbean.

2. Geodynamic setting

The Lesser Antilles Arc emplaced at the eastern boundary of the Caribbean Plate as a result of the west-southwestward subduction of North America and South America oceanic lithospheres, at a rate of around 2.0 cm/y (e.g. Deng and Sykes, 1995; Dixon et al., 1998; De Mets et al., 2000; Pindell and Kennan, 2009) (Fig. 1). The NW-SE trending Barracuda and Tiburon ridges are the diffuse plate boundary between North and South American plate (Fig. 1). These features accommodate the slow North and South America plate convergence and consist of oceanic fracture zones reactivated since the Middle Miocene, and the Pleistocene respectively (Patriat et al., 2011; Pichot et al., 2012). At La Désirade latitude, the subduction is orthogonal. The ridges trend oblique to the plate motion vector, thus sweeping the subduction zone from North to South at a rate of 2.0 cm/y. Nowadays, the topographic effect of the Tiburon ridge is observed across the outer fore-arc to the East of La Désirade Island (Figs. 1 and 2) (McCann and Sykes, 1984; Bouysse and Westercamp, 1990; Bangs et al., 2003; De Min et al., 2015). Northwestward of La Désirade, the Lesser Antilles trench curves and extends into the E-W Puerto Rico Trench. Northwardly, increasing subduction obliquity resulting from the trench curvature triggers strain partitioning in the upper plate that induced trench-parallel strike-slip combined with trench-parallel extension in the fore-arc (Bouysse and Westercamp, 1990; Feuillet et al., 2002; 2004; Laurencin et al., 2017; Legendre et al., 2018).

In the Guadeloupe archipelago fore-arc extensive tectonics is highlighted by two main E-W trending grabens: the Marie-Galante graben and the La Désirade graben (Fig. 2). The Marie-Galante graben is bounded to the North by the Basse-Terre Island, corresponding to the active volcanic arc, and by the Grande-Terre Island, corresponding to a tectonic high, and to the South, by the Marie Galante Island corresponding to a tectonic high. La Désirade Island is located on top of the hangingwall of the main southern border normal faults of the La Désirade graben. The La Désirade tectonic high extends to

98 the South into the submerged Karukéra spur that is the eastern border of the Marie-Galante basin.
99 The age and characteristics of this extensive tectonics and related fore-arc uplift are debated.

100 Based on the study of a flight of reef terraces, Feuillet et al. (2004) proposed that, since 330 ka, the
101 whole archipelago emerged, underwent a uniform uplift and regional westward tilting by 0.35°.
102 Following these authors, La Désirade, closest island to the trench, should have emerged since 330 ka
103 and then should have been more uplifted than other islands in relation with a westward tilting.
104 Feuillet et al. (2002) interpreted these features as trench-parallel extension linked to slip partitioning
105 along the northern part of the Lesser Antilles subduction zone. Feuillet et al. (2004) suggested that
106 the tilt probably resulted from a transient deformation episode at the subduction interface that
107 predated the late Pleistocene.

108 Based on the study of Pliocene-Pleistocene carbonate platforms, Cornée et al. (2012) and Münch et
109 al. (2013, 2014) evidenced that the emergence of islands of Guadeloupe archipelago occurred in the
110 1.07-1.54 Ma interval, i.e. 0.74 to 1.21 Ma earlier than proposed by Feuillet et al. (2004). Offshore,
111 De Min et al. (2015) showed that the Karukéra spur experienced three main extensional episodes (i.e.
112 Eocene?–Oligocene, Late Miocene and since Calabrian) with alternations between uplift and
113 subsidence periods. The main extensional directions evolved from NW–SE, E–W to N–S, respectively
114 (De Min et al., 2015). Since Calabrian, the Karukéra spur tilted to the east-northeast triggering
115 subsidence of the Eastern Flank (more than 2000 m) and emersion of both the northern part up to La
116 Désirade and the western flank of the spur (De Min et al., 2015).

117

118 **3. Geomorphology and geological setting**

119 La Désirade Island is 11.5 km long, 2 km large and reaches a maximum altitude of 276 m above sea
120 level (asl). The island consists of Jurassic to Cretaceous metamorphic basement capped by *ca* 120 m
121 thick Pliocene-Pleistocene carbonate platform deposits (e.g. Westercamp, 1980; Léticée, 2008;

Lardeaux et al., 2013; Münch et al., 2013; 2014). These carbonate platform deposits span the Zanclean–Calabrian interval (Léticée, 2008; Münch et al., 2013, 2014). The youngest deposits of this platform (1.54-1.07 Ma interval; Münch et al., 2014) correspond to a thick-branched *Acropora palmata* reef platform reaching a 10 to 15 m thickness at maximum (Fig. 4). These deposits occur near sea-level at Anse des Galets, Beauséjour at the western tip of the island, and at an elevation of 210 meters asl at the top of the eastern part of the island. These differences in elevation were triggered by a major episode of extensional tectonics accommodated by both N90°E and N110°E-N130°E normal faults, either during Ionian (Feuillet et al., 2004) or during Early Calabrian (Münch et al., 2014). This episode caused the emergence of Pliocene-Pleistocene carbonate platforms that now form the Upper Plateaus, and their local tilting (Lardeaux et al., 2013; Münch et al., 2014).

At La Désirade the amplitude of the tides is less than a meter (30 cm with a maximum from 50 to 60 cm) (e.g. BRGM, 2010). The northern coast of La Désirade is dominated by erosion and high and steep cliffs with few preserved raised beaches and coral reef terraces. On the southern coast of the island, sheltered from wind and swells by fringing reefs, uplifted beaches, coral reef terraces and wavecut surfaces are better preserved. There, a coral reef terrace corresponding to the Last Interglacial maximum has been studied and dated (Battistini et al., 1986; Feuillet et al., 2004). In the southwesternmost part of the island, at Pointe Frégule (Fig. 3A), U/Th ages on corals provided 119 ± 9 ka (Battistini et al., 1986, but ages were provided without U and Th concentrations, $^{234}U/^{238}U$ values, and $^{230}Th/^{232}Th$ values) and 141 ± 7 ka (Feuillet et al., 2004). In the northeastern part, at Baie-Mahault (Fig. 3A), Battistini et al. (1986) provided an age of 272 +72 to -43 ka.

Elsewhere in the Guadeloupe archipelago, Pliocene-Pleistocene carbonates platforms, named Upper Plateaus, are fringed by up to four mid-late Pleistocene coral reef terraces or wavecut surfaces, which were identified at Grande Terre and Marie Galante (de Reynal de Saint Michel, 1966; Westercamp, 1980; Battistini et al., 1986; Feuillet et al., 2004) (Fig. 2). In these islands, the lowermost terrace, at an elevation of 5-10 m asl, was dated from the 158 – 110 ka interval (Last

147 Interglacial Maximum terrace; Battistini et al., 1986; Feuillet et al., 2004). At Marie Galante, a second
148 uplifted marine terrace, occurring at an altitude ranging from 50 to 108 m asl, yielded a model age of
149 249 ka (terrace T2; Villemant and Feuillet, 2003; Feuillet et al, 2004). By correlating measured ages of
150 both marine terraces in Marie Galante with the SPECMAP isotopic curve, Feuillet et al. (2004)
151 proposed an age of 330 ka for the emersion of all islands of the archipelago.

152 We investigated La Désirade Island for datable uplifted marine erosional terraces (wavecut surfaces),
153 marine constructional terraces (coral reef) and depositional terraces (beaches) to analyse Pleistocene
154 vertical tectonic motions of the fore-arc.

155

156 **4. Methods**

157 *4.1. High-resolution mapping*

158 We conducted several field-mapping campaigns at 1/10000 scale, mapping with in detail wavecut
159 surfaces and marine terraces. Elevations and spatial extent of the terraces were determined using
160 field mapping, Garmin GPS and a 5m resolution DEM (Litto-3D Guadeloupe, V1, IGN-SHOM 2013).
161 Cross-sections were built using QGIS software (http://www.qgis.org) (Fig. 5). Elevation data are from
162 SHOM and function of the Present-Day mean sea level reference (uncertainty is ± 1m). Special
163 attention was devoted to the location of fossil strandlines, flat and subhorizontal terraces, beach
164 facies, notches, coral reefs, and shoreline angle (Lajoie, 1986; Pirazzoli et al., 1993; Montaggioni and
165 Braithwaite, 2009; Pedoja et al., 2011; Jara-Muñoz et al., 2015) (Fig. 5D). For the coral reef platform
166 (Upper Plateaus), the preserved faunal content allows an estimation of the paleo-bathymetry before
167 its emergence.

168 *4.2. U/Th Dating*

We made sure that the necessary conditions for using U-series ages of corals were meet by our samples: (i) few or no evidence of recrystallization, (ii) presence of little or no non-radiogenic ^{230}Th and (iii) initial $^{234}U/^{238}U$ value in agreement with modern seawater one (1.141 to 1.155; Delanghe et al., 2002). Corals selected for U/Th datations were first examined in thin-sections in order to select aragonite samples and avoid recrystallization or pore-infilling. We determine their mineralogy and quantify their aragonitic content by X-Ray diffraction at the University of Montpellier (Philips X'Pert PRO MPD diffractometer; PANalytical X'Pert HighScore Plus version 3.0.5 software). Each sample was analyzed during one hour between 5 and 60° Theta, with a 0.033° Theta step. We selected six samples that fulfil conditions and yield more than 95% of aragonite.

We carried out radiometric U/Th dating using the „*AXIOM*" MC-ICP-MS at IFM-GEOMAR Kiel, Germany. About 60 mg of carbonate powder drilled from each sample were dissolved (HNO_3), and 50 µl of a pre-mixed $^{229}Th/^{233}U/^{236}U$-spike solution ("*Mix9*") were added before evaporating the samples on hotplates at 90°C under filtered air. Dried samples were dissolved in 7n HNO_3 and passed through ion chromatographic columns containing 2 ml of EICHROM´s UTEVA® resin. After separation, two fractions (U and Th) were measured separately using the *MIC* (*M*ulti-*I*on-*C*ounting) method described by Fietzke *et al.* (2005). We controled the analytical quality by analyzing the reference standard (HU 1) and two blank samples. Secular-equilibrium standard HU-1 gained the $^{230}Th/^{234}U = 0.9989 \pm 0.0014$ and $^{234}U/^{238}U = 0.9994 \pm 0.0011$ activity ratios (95% confidence). Within the limits of uncertainty both isotope ratios match the reference values of 1. Analytical blanks are provided in Table 1. Being typically about 3-4 orders of magnitude lower than the respective sample amounts analytical blanks were practically insignificant but nevertheless data were blank-corrected. We corrected from the non-radiogenic ^{230}Th incorporated during carbonate formation using the following equation:

$$^{230}Th_{xs} = {}^{230}Th_{measured} - {}^{230}Th_{non\text{-}rad} = {}^{230}Th_{measured} - (0.7 \pm 0.2) * {}^{232}Th_{measured}$$

Where $^{230}Th_{xs}$ represents the excess amount of ^{230}Th produced by the decay of uranium.

4.3. Uplift rate determination

194 We assigned a sea-level highstand corresponding to a Marine Isoltopic Stage to each dated
195 paleoshoreline. Even if large uncertainties remain in estimating paleo-sea level during Pleistocene,
196 we use the long record of paleo-sea levels from Rohling et al. (2014) because it has been validated
197 from two independent methods: (i) deep-sea temperature changes from oxygen isotopes converted
198 into sea level and (ii) hydraulic control of water exchange through a narrow connection with the
199 open ocean in semi enclosed seas (Red Sea and Mediterranean). We give the paleo-sea levels with a
200 wide error margins for each isotopic stage, graphically calculated from the curve of Rohling et al.
201 (2014). Ages of the different interglacial MIS, even if sometimes debated, are the mean ages
202 provided by these authors. Results do not take into account isostatic correction. We estimate relative
203 vertical uplift between each paleoshoreline on the basis of the difference of elevations corrected
204 from paleo-sea levels of Rohling et al. (2014), and the morphostratigraphic model of Lajoie (1986)
205 and Saillard et al. (2009). This stratigraphic model has the following equation: Uplift rate
206 $interval_{Tn/Tn+1}$ = [(elevation of shoreline angle of $Terrace_n$ – elevation of shoreline angle $Terrace_{n+1}$) –
207 (Sea level at $MIS_{Terrace\ n}$ – Sea level at $MIS_{Terrace\ n+1}$)]/ (age of $MIS_{Terrace\ n}$ – age of $MIS_{Terrace\ n+1}$). This
208 equation allows us to propose apparent uplift rates between the formations of two successive
209 shoreline angles related to marine terraces.

210

211 **5.** Sedimentary facies, paleo-environments and new U/Th age of reefal units

212 *5.1. Acropora palmata reef platform (top of Upper Plateaus)*

213 The platform was uplifted at maximum to an elevation of 210 m asl and displays in growth position
214 massive coral colonies and locally thick-branched *Acropora palmata* colonies (Fig. 4C) and packstones
215 dominated by bivalves and benthic foraminifers (among which Amphisteginids). The general
216 sedimentological features of this unit are indicative of an inner reefal platform depositional
217 environment at very shallow water (Montaggioni and Braithwaite, 2009). Especially, the Caribbean
218 species *A. palmata* optimally lives between sea level and 5 m bsl (Veron, 2000) (Fig. 4D). Thus, we

219 considered in our calculations that the last unit of the Pliocene-Pleistocene carbonate platform was
220 deposited at ca 5 m below sea level (bsl).

221 *5.2 Depositional marine Terrace 1*

222 Terrace 1 was found in the northeastern part of the island as a 500 m wide subhorizontal erosional
223 relict between Pointe Adrien and Pointe du Grand Abaque. The metamorphic basement and the red
224 algal platform deposits are uncomformably oeverlaid by terrace 1 between 90 and 85 m asl (Fig. 3A
225 and 6A), corresponding to the 90 m asl littoral terrace of Lasserre (1961). Above the basement,
226 locally few dm-thick littoral limestones with pebbles are preserved, sometimes encrusted by red
227 algae (Fig. 6B) or bored by lithophagid molluscs. These pebbles are derived from both the
228 metamorphic basement and the Zanclean red algal carbonate platform. Limestones are packstones
229 with coral and oyster fragments, Amphisteginids, regular echinoids and red algae. Discrete notches
230 are locally preserved, carved into the Zanclean red algal carbonate platform deposits (Figs. 3A and
231 5A), and the shoreline angle is located at 90 ± 1 m asl. These deposits are indicative of a very shallow
232 littoral environment and were erroneously mapped as basal deposits of the Zanclean platform by
233 Westercamp (1980).

234

235 *5.3. Depositional marine Terrace 2*

236 The summit of the deposits of Terrace 2 correspond to foreshore deposits or coral buildups at 76 ± 1
237 m asl. These are only found in the eastern part of the island, along 4 km between Pointe Adrien and
238 Baie Mahault (Figs 3, 5 and 7A), corresponding to the 75 m asl littoral terrace of Lasserre (1961). At
239 Route de la Montagne, a well preserved 5 m thick marine terrace rests directly on the metamorphic
240 basement and its top is at 76 ± 1 m asl (Fig. 3A and 7B to E). From base to top, it contains: loose
241 pebbles, normally graded conglomerates with pebbles originating from the basement and the
242 Zanclean red algal platform, calcareous conglomerates bearing Amphisteginids and bioclastic
243 limestones with low-angle planar bedding are found in the uppermost part. These latter are

packstones to grainstones with benthic foraminifers (among which Amphisteginids), red algae, gastropods, bryozoans, corals and echinoids. Some coral fragments are coated with encrusting red algae (rhodoliths). Aragonitic *Diploria* coral colonies from the uppermost part of the deposits (Fig. 7E to G) yielded an age older than 500 ka (Sample DS 10-05; Table 2). Based only on the uranium isotope ratio it is possible to calculate a U/U apparent age of 659 -33 ka, +36 ka assuming an initial $^{234}U/^{238}U$ activity ratio of 1.146 (modern sea water).

All these deposits are indicative of a reefal to peri-reefal depositional environment in foreshore to uppermost shoreface setting (Tucker and Wright, 1990; Montaggioni and Braithwaite, 2009). They were deposited at the foot of a paleocliff transecting the Zanclean platform and the metamorphic basement. The summit of this depositional terrace, at 76 ± 1 m asl, is considered as a shoreline angle level. These deposits were erroneously mapped as basal deposits of the Zanclean platform (Westercamp, 1980).

5.4. Depositional marine Terrace 3

A subhorizontal wavecut surface is scarcely preserved 36 m asl all around the island (Figs. 3 and 5). This surface corresponds to the 35m asl terrace identified at the eastern tip of the island by Lasserre (1961). This wavecut surface is found transecting either the Zanclean red algal platform at Cap Frégule or the basement at Roche du large (Fig. 8D).

At Pointe Doublé, a depositional marine terrace was also identified (Lasserre, 1961). This terrace is topped by a flat surface at 36 ± 1 m asl and consists of 2.5 m thick karstified grainstones with planar laminations (Fig. 8C) that yielded rounded fragments of red algae, mollusks, Amphisteginids and few basement clasts. These deposits are considered as deposited in foreshore setting and their summit is interpreted as representing a shoreline angle.

At Cul Foncé, we evidenced a depositional marine terrace made of conglomerates and limestones and topped by a flat surface culminating at 36 ± 1 m asl surface (Fig. 8A and B). This terrace rest

against a cliff in the basement between 28 and 36 m asl above an erosion surface (Fig. 9A). In its lower part, occur conglomerates with cross-trough stratifications and planar bedding (Fig 9C). Pebbles are composed of diverse rocks that originate from both the basement and the Zanclean platform. Above, conglomerates evolve into bioclastic limestones with 3D dunes (Fig. 9B), low-angle parallel laminations (Fig. 9C and E), cross-stratifications (Fig. D) and locally hummocky cross-stratifications. Some broken massive coral colonies can be found (Fig. 9E, F).

These sediments were deposited into perireefal high energy depositional environment oscillating between foreshore and upper shoreface setting at the foot of a paleocliff (Fig. 8B). The summit of the foreshore deposits at 36 m ± 1 asl corresponds to the shoreline angle, and notches in the basement can be found at this elevation. The aragonitic coral sample DS10-40 yielded a U/Th age of 306 ± 6 ka, (Fig. 9, E and F; Table 2). These deposits were erroneously mapped as Zanclean carbonate platform deposits (Westercamp, 1980).

5.5. Coral reef Terrace 4

Coral reefs of Terrace 4 are well preserved and were previously identified (Lasserre, 1961; Battistini et al., 1986; Feuillet et al., 2004). This constructed terrace can be followed at an elevation between sea level (distal edge) and + 10 m asl (inner edge). The paleo-shoreline angle of this terrace was patchily reconstructed all around the island based on scattered but abundant exposure at 10 m asl: between Baie Mahault and Le Souffleur (Fig. 4A), Cul Foncé (Fig. 8A), Cap Frégule (Fig. 10), Airport quarry, Pointe Fromager (Fig. 11) and Pointe Mancenillier (Fig. 12F). We detail here only the locations where we were able to perform U/Th datings.

At Baie Mahault (Fig. 12A) massive to columnar corals, mainly *Montastraea* (Fig. 12A and E) associated with *Diploria* and *Porites*, are cropping out landwards whereas *A. palmata* boundstones and *Strombus* accumulations are abundant seawards (Fig. 12, A, D, E). The summit of the deposits is gently dipping (0.5 to 1°) seawards from 10 m to 4 m asl. At the top of the preserved reef deposits is a tens of cm-thick level displaying thin-branched *Acropora* at 5 m asl (Fig. 12A and B). These corals

yielded an age at 133.5 ± 0.84 ka (Sample DS 11-43, Fig.12A to C; Tab. 2). This age is much younger and precise than the one previously published, i.e. 272 +72 to -43 ka (Battistini et al., 1986), and we considered that our new age as the estimate for Terrace 4. The Terrace T4 corresponds to a fringing reef complex in high-energy shallow-water environments, deposited on a seaward low-angle dipping ramp.

In the southwestern part of the island the reef complex comprises large colonies of *A. palmata*, *Montastraea* and *Diploria* in growth position and coral rubbles and coarse-grained bioclastic limestone with *Strombus*. This complex gently dips to the West, from 10 m asl at Airport Quarry to sea level at Cap Frégule and Pointe Colibri. We performed U/Th dating at 2.5 m asl at Pointe Frégule (Fig. 10F and G). Two aragonitic coral colonies, *A. palmata* (DS 10-12a) and *Montastraea* sp. (DS10-12b) provided ages, 126.09 ± 0.58 ka and 128.19 ± 0.61, respectively (Fig. 3 and Table 2). These results are in good agreement with the age we obtained for the Terrace 4 in Baie Mahault and with those previously obtained at Pointe Colibri (Battistini et al., 1986; Feuillet et al., 2004).

6. Discussion

6.1 Ages used for the uplift rates calculation

Some uncertainties remain concerning the ages of terraces 1 and 2. However, we proposed here estimate based on the U/Th ages of terraces 3 and 4 and the estimated age of the *A. palmata* coral platform. We correlated each terrace with the paleo-sea level curve from Rohling et al. (2014) and one or several Marine Isotopic Stage highstand (Fig. 13).

Terrace 4 yielded ages ranging between 126-133 ka, indicating that the 10 m asl paleoshoreline formed during the the Last Interglacial Maximum highstand (MIS 5e) dated at 122 ka. Terrace 3 yielded an age of 305.76 ± 5.96 ka, indicating that the shoreline angle at 36 ± 1 m asl formed during the 310 ka MIS 9 highstand. Terrace 2 yielded an age of 659 -33 ka, +36 ka, indicating that the shoreline angle at 76 m may have formed during the MIS 15 high sea level at 620 ka or the during the

317 MIS 17 one at 700 ka. In Grande Terre, the *A. palmata* reef platform deposited during the reverse
318 subchron C2r, in the 1.07-1.54 Ma interval (Münch et al., 2014). This platform deposited
319 synchronously in La Désirade and in Marie Galante (Cornée et al., 2012; Münch et al., 2013, 2014).
320 This interval includes two main highstands: MIS 31 at 1.07 Ma and MIS 47 at 1.48 Ma (Fig. 13).

321 As a consequence, the age of Terrace 1 is bracketed by the estimated ages range for Terrace 2,
322 correlated with MIS 15 or MIS 17 highstands, and the age range of *A. palmata* reef platform (MIS 31-
323 47 interval). Consequently, we considered that Terrace 1 was formed in a time span ranging from the
324 high sea-levels MIS 19 to 25, *i.e.* in the 780 to 970 ka taking into account the youngest age (1.07 Ma)
325 for the *A. palmata* reef platform (Fig. 13). However the incertitude on the age of the Terrace 1 could
326 be much greater taking into account an older age for the *A. palmata* reef platform.

327 *6.2. Pleistocene vertical motions in the northern Lesser Antilles fore-arc*

328 In the Guadeloupe Archipelago, apart from La Désirade, uplifted Pleistocene marine terraces also
329 crop out in Grande Terre and Marie Galante. In Grande Terre, only the Last Interglacial Maximum
330 terrace was recognized at an elevation between 0.5 and 6 m asl and was dated between 149 and 158
331 ka (Battistini et al., 1986; Feuillet et al., 2004) (Fig. 14). In Marie Galante, a flight of four uplifted
332 Pleistocene marine terraces was described but only the lowermost one, at an elevation between 2
333 and 15 m asl, was dated accurately between between 110 and 134 ka (Battistini et al., 1986; Feuillet
334 et al., 2004). A modeled age at 249 ± 8 ka was also proposed for a second terrace on Marie Galante
335 that is the second most elevated at 50–108 m asl (T2 *in* Feuillet et al., 2004). This age was calculated
336 in an open system to account for selective mobilities of U-series isotopes in a partly recrystallized
337 (calcite) coral sample (Villemant and Feuillet, 2003). Uplifts are related to a westward tilting and/or
338 local deformation along normal faults bounding the Marie Galante graben. Local deformations result
339 in a lowering of the terraces elevation towards the center of the graben whereas westward tilting of
340 the Marie Galante Island results in higher uplift in the eastern part of the island. In Marie Galante, an
341 uplift rate was calculated for the Last Interglacial Maximum terrace at 0.08 mm/yr (Feuillet et al.,

2004). The same authors also calculated higher uplift rates (0.2 mm/yr) taking into account an age of 330 ka for the *A. palmata* reef platform (Upper Plateaus) based on the correlation of both dated terraces with the SPECMAP curve. However, the reverse magnetic polarity of the *A. palmata* reef platform (Münch et al., 2014) contradicts the estimated age used for uplift rate calculations and questions the validity of the modeled age of Villemant and Feuillet (2003) for the second most elevated terrace in Marie Galante. As we found an age of 659 -33 ka, +36 ka for T2 (the second most elevated terrace) and 306 ± 6 ka for T3 in La Désirade, the age of the *A. palmata* reef platform is definitely not 330 ka. Thus, only the mean uplift rate of 0.08 mm/yr for the MIS 5 terrace in Marie Galante can be considered valid.

In Saint Martin, only the MIS 5 terrace was described and crops out at ca 12 m asl and, in Puerto Rico, the MIS 5 terrace is between 4.5 and 5.5 m asl (synthesis in Pedoja et al., 2014) (Fig. 1). In the Dominican Republic, the MIS 5e terrace is between 10 and 20 m asl (Diaz de Neira et al., 2015).Thus, the uplift of the MIS 5 terrace appears to be limited in the northern Lesser Antilles fore-arc whereas it reaches ca 60 m asl in the southern Lesser Antilles forearc, in the Barbados Island, where the highest MIS 11 shoreline angle was found between 120 and 140 m asl (Speed and Cheng, 2004). This highlights the specificity of La Désirade, one of easternmost islands of the fore-arc, where can be depicted vertical motions and deformations of the fore-arc since 1.5 Ma.

6.3 Uplift rates at La Désirade

6.3.1. Post -Terrace 4 uplift

During MIS 5e the sea level was estimated at 2 to 8 m asl (Kopp et al., 2009; Murray-Wallace and Woodroffe, 2014; Rohling et al., 2014; Creveling et al., 2015) and the paleo-shoreline is presently at 10 m ± 1 asl. Thus, Terrace 4 experienced 2 ± 1 to 8 ± 1 m uplift since 122 ka taking into account uncertainties on paleo-sea level during MIS 5e (Fig.13A). Apparent uplift rates range from 0.008 to 0.07 mm/y. Such rates are very low, especially for an active tectonic setting (Sieh, 1999; Henry et al., 2014; Saillard et al., 2017). As the estimated paleo-shoreline angle from the top of Terrace 4 remains

367 at the same elevation around the island, the island underwent a uniform and very slow uplift after
368 MIS 5e without any significant tilting.

369 *6.3.2. Uplift between Terrace 3 and Terrace 4*

370 The paleo-shoreline angle of the MIS 9 deposits is at 36 ± 1 m asl and dates 310 ka. At this time, the
371 high sea level was estimated between 0 and 6 m asl (Rohling et al., 2014) (Fig. 13). The difference in
372 elevation between MIS 5e and MIS 9 high sea levels is 2 to 8 m. As a consequence, the MIS 9
373 paleosea level underwent 28 ± 1 to 34 ± 1 m (27m at minimum to 35m at maximum) uplift before the
374 formation of the MIS 5e coral reef at 122 ka. This uplift occurred during a time span lasting 188 ka,
375 indicative of apparent uplift rate ranging from 0.14 to 0.19 mm/y. Even if low, this rate is much
376 greater than the post MIS 5e rate. The mean uplift rate of Terrace 3 in reference to the Present-Day
377 sea level (36 ± 1 minus 0 to 6 m during 310 ka) is in the interval 0.11 to 0.14 mm/y. It is to note that
378 the Terrace 3 is scarcely preserved but found all around the island at the same elevation, thus
379 indicating the lack of tilting since 310 ka.

380 *6.3.3. Uplift between Terrace 2 and Terrace 3*

381 The shoreline angle of Terrace 2 is at 76 ± 1 m asl. During MIS 15 to 17 the high sea levels were
382 estimated to be 10 m bsl to 22 m asl (Rohling et al., 2014). The difference in elevation between
383 Terraces 2 and 3 is 40 ± 1 m. The uplift between MIS 15-17 and MIS 9 is thus in the 18 ± 1 to 50 ± 1 m
384 interval in a time range of 310 ka minimum to 390 ka maximum. The apparent uplift rate is thus
385 estimated in the 0.04–0.16 mm/y interval. The mean uplift rate of Terrace 2 in reference to the
386 Present-Day sea level ranges between 0.14 and 0.28 mm/y.

387 *6.3.4. Uplift between Terrace 1 and Terrace 2*

388 The shoreline angle of Terrace 1 is at 90 ± 1 m asl and may correspond to MIS 19 or 21 or 25 high sea
389 levels. The lowest and highest elevation of sea level for this time interval are estimated 5 m bsl and
390 19 asl, respectively (Rohling et al., 2014) (Fig. 13). The difference in elevation between terraces 1 and

391 2 is 14 ± 1 m. The extreme net values of uplift and subsidence are thus + 19 to – 7 m, respectively.
392 The time range of the uplift lasted from MIS 17 to MIS 25 at maximum (270 ka), from MIS 17 to MIS
393 19 at minimum (80 ka). We estimate that the vertical motion rate is ranging between ca 0 and + 0.24
394 mm/y. The mean uplift rate of Terrace 1 in reference to the Present-Day sea level (90 m elevation
395 minus 19 m or plus 5 m paleosea level during 80 ka minimum and 270 ka maximum) is in the interval
396 0.26 to 1.2 mm/y.

397 *6.3.5. Mean uplift rate of the A. palmata reef platform*

398 We calculate only mean uplift rate in reference to the Present-Day sea level for *the A. Palmata* reef
399 platform because of large uncertainties on its age and the age of Terrace 1. In the northeastern part
400 of the island, east of the Coulée du Grand Nord Fault and east of Le Souffleur Fault, the summit of
401 the coral platform crops out at 210 m asl at maximum (Fig. 3). In the western part of the island, the
402 platform was lowered later by the activity of main N40° and N130° trending normal faults. The
403 occurrence of large colonies of *A. palmata* in growth position is indicating a paleobathymetry of 5 m
404 at the end of deposition (Fig. 4). The minimum and maximum ages of the coral platform are those of
405 the highest sea level MIS 31 (1.07 Ma) and MIS 47 (1.48 Ma), respectively. During MIS 31 and MIS 47
406 sea level was estimated between 5 to 47 m asl (Rohling et al., 2014). The mean apparent uplift rate
407 of the coral platform in reference to the Present-Day sea level is in the range of 0.84–2.00 mm/y.

408 *6.3.6. Global trend of apparent uplifts at La Désirade*

409 The mean uplift rates at La Désirade, calculated in reference to the Present-Day sea level, are
410 decreasing since the *A. palmata* reef platform emergence (Fig. 13). Large uncertainties on the age of
411 the platform and the Terrace 1 do not allow precise comparison. However, the large difference in
412 uplift amplitude between the platform and Terrace 1 suggests that a severe slowing occurred after
413 the emergence of the platform. This is also suggested if only minimum uplift rate values are taken
414 into account. During the period corresponding to the terraces deposition and uplift, mean uplift rates
415 continued to decrease from 0.26-1.19 mm/y since the MIS 19-25 interval to 0.008-0.07 mm/y since

MIS 5e. This decrease is confirmed since Terrace 2 deposition, from 0.14-0.28 mm/y to 0.008-0.07 mm/y to Present-Day. Thus, La Désirade was uplifted since the *A. palmata* reef platform deposition, and uplift decreased at last since 310 ka to become negligible since 122 ka but we favour a major decrease in uplift rates after the platform emersion.

6.4 Vertical motion and geodynamics in the Guadeloupe fore-arc since 1.5 Ma

6.4.1. Pleistocene fore-arc tectonics

The Pleistocene to Present-Day fore-arc tectonics at the latitude of the Guadeloupe has been described mainly as submeridian extension accommodated by E-W normal faults (Feuillet et al., 2004). This extensional tectonics has been considered coeval with a local west- southwestward tilting of Marie Galante Island. On La Désirade and offshore, on the Karukéra spur (SE of La Désirade), a north-northeast direction of extension, oblique to the fore-arc trend, reactivates the inherited N180° to N130° and N70° to N50° trending faults and is accommodated by the development of N90° trending ones in the central part of the spur (Corsini et al., 2011; Lardeaux et al., 2013; Münch et al., 2014; De Min et al., 2015). It is to note that the fore-arc basement, which is cropping out in La Desirade only, is strongly deformed and its structure results from 140 Ma of geological evolution of the Caribbean plate (Lardeaux et al., 2013). De Min et al. (2015) also showed that 1/ a differential subsidence of the Karukéra spur occured since the Oligocene, and went on during the Pleistocene, in relation with the activity of the major N70° normal fault, north of La Désirade, and 2/ a major eastward or trenchward tilting affected the Karukéra spur during the Pleistocene. This tilting (Fig. 15) was evidenced by differential erosion of Late Pliocene/Early Pleistocene drowned coral reefs which were severely eroded on the northern and western parts of the spur and preserved on the eastern flank (De Min et al., 2015). This tilting is synchronous with the reactivation of N130°E-striking normal faults on the spur (De Min et al., 2015). In La Désirade, we found that the *A. palmata* reef platform is mainly preserved in the easternmost part of the island, i.e. in the hanging wall of La Coulée du Grand Nord N130°E-striking normal fault. In the western part of this compartment, uppermost units of the

platform poorly crop out and the *A. Palmata* reef platform is only locally preserved in the hanging walls of N40°E-striking normal faults and is eroded elsewhere. Thus, the distribution of the preserved parts of the *A. palmata* reef platform is interpreted as indicative of an early Pleistocene eastward tilt coeval with the one observed offshore on the Karukéra Spur and with an extensional tectonic episode.

We evidenced that Terrace 3 and 4 on La Désirade occur at constant elevation all around the island (Figs. 3, 5 and 14), indicating that the activity of the N130°E and N70°E fault systems, crosscutting the island and responsible for a large offset of the *A. palmata* reef platform, occurred prior to T3 deposition (310 ka). As Terraces 1 and 2 were identified only in the northeastern part of the island, it is difficult to say whether they were affected by fault activity. However, insofar Terraces 1 and 2 remain at rather constant elevation along several kilometers they do not look affected by the observed brittle deformation and tilting of the *A. palmata* reef platform (Fig. 14). Moreover, the mean uplift rates decreased severely after the uplift of the *A. palmata* reef platform. Thus, we propose that the N70° and N130°E-striking normal fault activity and eastward tilting, coeval with the uplift of the *A. palmata* reef platform, ceased mainly before Terrace 1 deposition (0.78–0.97 Ma) and after the platform (1.07–1.54 Ma) deposition, *i.e.* during the Emilian–Sicilian interval.

The last Interglacial Maximum terrace (Terrace 4 in La Désirade) is affected by N90°E and inherited N130°-striking normal faults mainly in the innermost part of the fore-arc, on Marie Galante and Grande Terre, but also in the central-western part of the Karukéra spur. Onshore, this terrace is lowered by recent (e.g. the Barre de l'île fault system in Marie Galante) and active (e.g. Gosier fault in southern Grande Terre) faults toward the center of Marie Galante and Grippon plain grabens (Fig. 15, D). However, it remains at +5 m asl in eastern and northern Grande Terre, thus indicating the lack of post MIS 5 faulting and tilting in these areas.

At the scale of the archipelago, the organization of marine terraces is different along the coasts of different islands and thus cannot result of a single regional process. We rather evidenced two major

deformation episodes during the last 1.5 Ma. A first one occurred after the *A. palmata* reef platform and before the Terrace 1 deposition (Emilian–Sicilian interval) (Fig. 15, A and B), characterized in the eastern part of the archipelago by a trenchward tilting and localized uplift in relation mainly with the reactivation of N130°E inherited structures during a submeridian extensional episode. The second event started since 0.78 – 0.97 Ma and is still active (Fig. 15 C and D), and is characterized by the formation of E-W normal faults and the reactivation of N130°-striking normal faults, by differential uplift of Pleistocene marine terraces and by a southwestward tilting of the Marie Galante island.

6.4.2. Geodynamic implications

Over the last 5 My, the 2km high oblique-to-the-trench Tiburon ridge was subducted from North to South along the Lesser Antilles trench (Bangs et al., 2003; Patriat et al., 2011; Pichot et al., 2012). This ridge corresponds to the western end of the North America-South America diffuse plate boundary and its topography has been built in the middle-late Miocene-early Pleistocene (Patriat et al., 2011; Pichot et al., 2012). During the 1.5-1 Ma interval, it was located below the northern tip of the Karukéra spur, 25 km east of La Désirade (Fig. 15B). La Désirade is the easternmost emerged promontory of the inner fore-arc extending southeastwards to the immerged Karukéra spur (Fig. 2) that recorded a long-term regional extensional tectonics affecting the pre-structured fore-arc basement and cover and reactivating structural Mesozoic inheritance (Lardeaux et al., 2013; De Min et al., 2015). Along the Peru-Chile subduction zone, long-term permanent coastal uplifts coincide with areas of aseismic creep on the subduction interface promoted by the subduction of ridges or fracture zones (Saillard et al., 2017). Henry et al. (2014) showed that main parameter explaining coastal uplift is small-scale heterogeneities of the subducting plate as aseismic ridges. The magnitude and rate of coastal uplifts in fore-arcs do not appear correlated with the main geodynamics parameters. Thus we interpret the coastal uplift of the fore-arc at La Désirade to be related to the subduction of the Tiburon aseismic ridge. We propose that fore-arc uplift at the latitude of the Guadeloupe might reflect a change in frictional properties along the subduction

interface persisting over a million year related to the subduction of the Tiburon ridge. In addition, it is to note that subduction of aseismic ridges may also lead to fore-arc subsidence interrupted by rapid uplift episodes (Clift and Vanucchi, 2004; Vannucchi et al., 2013). This is in accordance with the long-term subsidence of the fore-arc at the latitude of the Guadeloupe archipelago, that is related to extensional tectonics in the fore-arc and that was interrupted by at least two major uplift episodes: one in late Pliocene and one in Calabrian times (Münch et al., 2014; De Min et al., 2015). The latter corresponds to the emersion of the *A. palmata* reef platform between 1.48–1.07 Ma in La Désirade and was also evidenced onshore and offshore throughout the archipelago (Cornée et al., 2012; Münch et al., 2013, 2014; De Min et al., 2015). Since 0.78–0.97 Ma (Sicilian), uplift went on at La Désirade but with low uplift rates despite its location close to the trench and the elevated slab dip (60°). Indeed, these two parameters have been shown to correlate with higher uplift rates, especially in accretionary convergent margins (Henry et al., 2014). Higher uplift rates were also evidenced in neighboring Caribbean areas with either compressive (Barbados, Gomez et al., 2018) or transpressive (western Hispaniola and Puerto Rico, Mann et al., 1995) fore-arc tectonics but these areas correspond to different tectonic regime of the subduction zone, accretional frontal subduction for the southern Lesser Antilles and oblique subduction in Hispaniola. The low uplift rates we evidenced in La Désirade are coeval with the N-S extensional tectonics of fore-arc. Such low uplift may rather correspond to erosional convergent margins (Henry et al., 2014). This is also supported by the presence of both numerous trenchward dipping normal faults within the Karukéra spur and Cenozoic carbonate platform sediments down the slope and close to the prism (De Min et al., 2015). Thus we propose that both extensional tectonics and low uplift rates in the Guadeloupe fore-arc exemplify the erosional character of the Lesser Antilles subduction zone since ~1 Ma in its central part (Bangs et al., 2003; Münch et al., 2014; De Min et al., 2015) although geologic and tectonic processes included accretion to form a frontal prism during former history of the central Lesser Antilles subduction zone. Such varying erosional *vs* accretional character along subduction zones has already been shown in relation with the subduction of asperities in different places (e.g. Aleutian; Von Huene et al., 2012).

We also evidenced a marked decrease of mean uplift rates after the emersion *A. palmata* reef platform in La Désirade and a continuous decrease of uplift rates until Present-Day. The high magnitude of the uplift of the platform and the higher uplift rates of the terraces were clearly coeval with a Calabrian extensional tectonic episode, and both may be the surficial expression of the subduction of the Tiburon ridge at the latitude of La Désirade. Bangs et al. (2003) showed that the backstop was deformed by the subduction of the Tiburon ridge, allowing sediments of the accretionnary prism to subduct. At Present-Day the Tiburon ridge is no longer located beneath La Désirade, but beneath the northern tip of the Karukéra spur *sensu lato* (Fig. 15D). This highlights that the major Calabrian uplift, with high uplift rates, was related to a transient event at the subduction interface provoking deep (backstop; Bangs et al., 2003) and surficial deformations. The vicinity of the trench may have enhanced the strong vertical motion (Henry et al., 2014). Later, the moderate uplifts cannot be directly related to this transient event and may have been controlled by various parameters of the subduction zone, e.g. the high deep slab dip, the extensional tectonics of the overriding plate and the erosional regime of the subduction.

At Present-Day the Lesser Antilles subduction zone is known to be moderately seismically active compared to other subduction zones in the world, showing (i) only few earthquakes with a magnitude greater than 7 along the megathrust (Ruiz et al., 2013) and (ii) most of the seismic activity clusters along the active volcanic arc within the Caribbean upper plate (< 50 km depths) (Christeson et al., 2003; Evain et al., 1013; Laigle et al., 2013). Moreover, at the latitude of the Guadeloupe, supra-slab earthquakes with normal-faulting seismic activity above 50km depth were recorded whereas deeper flat-thrust earthquakes were not observed (Laigle et al., 2013). These observations may be consistent with low seismic coupling (aseismic creep) at the subduction interface. Indeed, it has been proposed that the subduction of aseismic ridges provides fluids that can lubricate the subduction interface in turn promoting aseismic creep along the megathrust or enhancing small earthquakes occurrence (Chlieh et al., 2008; Schlaphorst et al., 2016; Saillard et al., 2017). Fluids may

also be responsible for high serpentinization of the supraslab mantle beneath the northern Lesser Antilles arc as proposed by Gailler et al. (2017).

7. Conclusion

In La Désirade, four shorelines angles were identified between 0 and 90 asl. They are associated with sediments deposited in shallow marine environment and coral reef depositional settings. The deposits of the terraces rest unconformable on both the basement and the Pliocene to early Pleistocene red algal and coral reef carbonate platform (Upper Plateaus) indicating a post-platform deposition eastward tilt. Aragonite corals from the three lowest terraces provided U/Th ages allowing to establish a new age model: Terrace 4 (+ 10 m) dates MIS 5e, Terrace 3 (+36 m) dates MIS 9, Terrace 2 (+ 76 m) is MIS 15 or MIS 17, Terrace 1 (+ 90 m) dates in the MIS 17 – 25 interval and the coral reef platform dates in the MIS 31 - 49 interval. Integrating U/Th dating and corrections of paleo-sea level and paleobathymetry of the studied platforms and terraces allow us to provide estimates of the apparent uplift rate at different times since ~1.5 Ma. During Early Calabrian (1.07-1.5 to 0.78-0.96 Ma interval) the Upper Plateaus recorded transient deformation accommodated by NW-SE and ENE-WSW trending normal fault systems. The mean uplift rate was high, in the 0.84-2.00 mm/y range. Then, since late Calabrian to Present-Day, uplift rates decreased from 0.26 mm/y at least to 0.008 to 0.07 mm/y. This decrease is peculiarly well documented since 310 ka. The large early Calabrian uplift appears to be related to the influence of the subducting, 2 km high oceanic Tiburon Ridge which reached the subduction interface below the northern Karukéra Spur near 1.5 Ma ago. Later, the ridge entered deeper into the mantle and its influenced vanished. The decreasing uplift rates then are related to other parameters of the subduction zone like the dip of the deep of the slab or the basal erosion of the upper plate or the extensional reactivation of Cretaceous structures related to ancient history of the basement.

Acknowledgments

This study was funded by the French National INSU Programs DyETI and SYSTER, the European Interreg IIIB 'Caribbean Space' and FEDER (op.30-700) projects as well as by the Region Guadeloupe and the French ANR GAARANTI. B. Fraisse performed the RX diffraction analysis (Réseau de Rayons X et Gamma Z, Ressource technologique de l'Université de Montpellier), D. Delmas and C. Nevado are thanked for thin-sections (Géosciences Montpellier). K. Pedoja (Caen University) is thanked for improvement of the manuscript. P. Mann and D. Fernandez Blanco are thanked for their reviews.

References

1. Bangs, N.L., Christeson, G.L., and Shipley, T.H., 2003. Structure of the Lesser Antilles subduction zone backstop and its role in a large accretionnary system. Journal of Geophysical Research, 108, 2358.

2. Barnes, P.M. and Nicol, A., 2004. Formation of an active thrust triangle zone associated with structural inversion in a subduction settings, eastern New Zealand. Tectonics, 23, TC1015.

3. Battistini, R., F. Hinschberger, C. T. Hoang, and Petit, M., 1986. La basse Terrasse corallienne (Eémien) de la Guadeloupe : morphologie, datation 230Th/ 234U, néotectonique. Rev. géomorph. dyn., XXXV, 1-10. https://www.researchgate.net/publication/291766951_The_Pleistocene_Eemian_low_coral_terrace_of_Guadeloupe_morphology_Th230U234_dating_neotectonics

4. Bouysse, P., and Westercamp, D., 1990. Subduction of Atlantic aseismic ridges and Late Cenozoic evolution of the Lesser Antilles island-arc. Tectonophysics, 175, p. 349, p. 357-355-380.

5. Bouysse, P., Garrabé, F., Maubussin, T. and Andreieff, P. , 1993. Carte géologique du département de la Guadeloupe : Marie Galante et les îlets de Petite Terre) 1/50000, Service Géologique National edn., BRGM, Orléans, France.

6. BRGM, 2010. Evolution et dynamique du trait de côte de l'archipel guadeloupéen. BRGM/RP-58750, Final Report, Orléans (F), 93pp.

7. Chappell, J., 1974. Geology of Coral Terraces, Huon Peninsula, New Guinea: A Study of Quaternary Tectonic Movements and Sea-Level Changes. Bulletin of the Geological Society of America, 85, 553-570.

8. Clift, P.D., and Vannucchi, P., 2004. Controls on tectonic accretion versus erosion in subduction zones: Implications for the origin and recycling of the continental crust. Reviews of Geophysics, 42, RG2001.

9. Chlieh, M., Avouac, J. P., Sieh, K., Natawidjaja, D. H., and Galetzka, J., 2008. Heterogeneous coupling of the Sumatran megathrust constrained by geodetic and paleogeodetic measurements. Journal of Geophysical Research: Solid Earth, 113(B5).

10. Christeson, G. L., Bangs, N. L., and Shipley, T. H., 2003. Deep structure of an island arc backstop, Lesser Antilles subduction zone. Journal of Geophysical Research: Solid Earth, 108(B7).

11. Collot, J.-Y. and Fisher, M.A., 1989. Formation of fore-arc basins by collison between seamounts and accretionary wedges: An example from the New Hebrides subduction zone. Geology, 17, 930-933.

12. Cornée, J.J., Léticée, J.L., Münch, P., Quillévéré, F., Lebrun, J.F., Moissette, P., Braga, J.C., Melinte-Dobrinescu, M., De Min, L., Oudet, J. and Randrianasolo, A., 2012. Sedimentology, palaeoenvironments and biostratigraphy of the Pliocene-Pleistocene carbonate platform of Grande- Terre (Guadeloupe, Lesser Antilles fore-arc). Sedimentology, 59, 1426-1451.

13. Corsini, M., Lardeaux, J.M., Vérati, C., Voitus, E. and Balagne, M., 2011. Discovery of Lower Cretaceous synmetamorphic thrust tectonics in French Lesser Antilles (La Désirade Island, Guadeloupe): Implications for Caribbean geodynamics. Tectonics, 30, TC4005.

14. Creveling, J.R., Mitrovica, J.X., Hay, C.C., Austermann, J. and Kopp, R.E., 2015. Revisiting tectonic corrections applied to Pleistocene sea-level highstands. Quaternary Science Reviews, 111, 72-80.

15. DeMets, C., Jansma, P.E., Mattioli, G.S., Dixon, T.H., Farina, F., Bilham, R.G., Calais, E. and Mann, P., 2000. GPS geodetic constraints on Caribbean-North America plate motion. Geophysical Research Letters, 27, 437-440.

16. Delanghe, D., Bard, E., Hamelin, B., 2002. New TIMS constraints on the uranium-238 and uranium-234 in seawaters from the main ocean basins and the Mediterranean Sea. Marine Chemistry, 80, 79–93.

17. De Min L., Lebrun, J.F., Cornée, J.-J., Munch, P., Léticée J.-L., Quillévéré, F., Melinte-Dobrinescu, M., Randrianasolo A., Marcaillou, B. and Zami, F., 2015. Tectonic and sedimentary architecture of the Karukéra spur: A record of the Lesser Antilles fore-arc deformations since the Neogene. Marine Geology, 363, 15-37.

18. Deng, J. and Sykes, L.R., 1995. Determination of Euler pole for contemporary relative motion of Caribbean and North American plates using slip vectors of interplate earthquakes. Tectonics, 14, 39-53.

19. de Reynal de Saint Michel, A., 1966. Carte géologique de la France et notice explicative, département de la Guadeloupe, feuilles de St Martin, St Barthelemy et Tintamarre, Basse-Terre et les Saintes, Marie-Galante et La Désirade, scale 1/50,000, Ministère de l'Industrie, Paris.

20. Diaz de Neira, J.A., Braga, J.C., Mediato, J., Lasseur, E., Monthel, J., Hernaiz, P.P., Pérez-Cerdan, F., Lopera, E. and Thomas, A., 2015. Plio-Pleistocene paleogeography of the Llanura Costera del Caribe in eastern Hispaniola (Dominican Republic): interplay of geomorphic evolution and sedimentation. Sedimentary Geology, 325, 90-105.

21. Dixon, T.H., Farina, F., Demets, C., Jansma, P., Mann, P. and Calais, E., 1998. Relative motion between the Caribbean and North American Plates and related boundary zone deformation from a decade of GPS observations. Journal of Geophysical Research, 103, 15157-15182.

22. Dominguez, S., Lallemand, S., Malavieille, J. and von Huene, R., 1998. Upper plate deformation associated with seamount subduction. Tectonophysics, 293, 207-224.

23. Dominguez, S., Malavieille, J. and Lallemand, S.E., 2000. Deformation of accretionary wedges in response to seamount subduction: insights from sandbox experiments. Tectonics, 19, 182-196.

24. Evain, M., Galve, A., Charvis, P., Laigle, M., Kopp, H., Bécel, A., Weinzierl, W., Hirn, A., Flueh, E.R., Gallard, J. and the Lesser Antilles Thales scientific party, 2013. Structure of the Lesser Antilles

subduction forearc and backstop from 3D seismic refraction tomography. Tectonophysics, 603, 55-67.

25. Feuillet, N., Manighetti, I., Tapponnier, P., and Jacques, E., 2002. Arc parallel extension and localization of volcanic complexes in Guadeloupe, Lesser Antilles. Journal of Geophysical Research: Solid Earth, 107, ETG 3-1–ETG 3-29.

26. Feuillet, N., Tapponnier, P., Manighetti, I., Villemant, B., and King, G.C.P., 2004. Differential uplift and tilt of Pleistocene reef platforms and Quaternary slip rate on the Morne-Piton normal fault (Guadeloupe, French West Indies). Journal of Geophysical Research: Solid Earth, 109, B2.

27. Fietzke, J., Liebetrau, V., Eisenhauer, A. and Dullo, W.-C., 2005. Determination of uranium isotope ratios by multi-static MIC-ICP-MS: method and implementation for precise U-and Th-series isotope measurements. Journal of Analytical Atomic Spectrometry, 20, 395-401.

28. Gailler, L.S., Mertelet, G., Thinon, I., Bouchot, V., Lebrun, J.-F. and Münch, P., 2013. Crustal structure of Guadeloupe islands and the Lesser Antilles Arc from a new gravity and magnetic synthesis. Bulletin de la Société Géologique de France, 184, 77-97.

29. Gailler, L., Arcay, D., Münch, P., Martelet, G., Thinon, I., and Lebrun, J.-F., 2017. Forearc structure in the Lesser Antilles inferred from depth to the Curie temperature and thermo-mechanical simulations. Tectonophysics, 706-707, 71-90.

30. Gomez, S., Bird, D. and Mann, P., 2018. Deep crustal structure and tectonic origin of the Tobago-Barbados ridge. Interpretation, 6, T471-T484.

31. Gutscher, M.A., Kukowski, N., Malavieille, J. and Lallemand, S.E., 1998. Episodic imbricate thrusting and underthrusting; Analog experiment and mechanical analysis applied to Alaskan accretionary wedge. Journal of Geophysical Research: Solid Earth, 103, 10161-10176.

32. Henry, H., Regard, V., Pedoja, K., Husson, L., Martinod, J., Witt, C. and Heuret, A., 2014. Upper Pleistocene uplifted shorelines as tracers of (local rather than global) subduction dynamics. Journal of Geodynamics 78, 8-20.

33. Jara-Munoz, J., Melnick, D. and Strecker, M. R., 2015. TerraceM: A MATLAB® tool to analyze marine and lacustrine terraces using high-resolution topography. Geosphere, 12, doi: 10.1130/GES01208.1.

34. Kopp, R. E., Simons, F. J., Mitrovica, J. X., Maloof, A. C. and Oppenheimer, M., 2009. Probabilistic assessment of sea level during the last interglacial stage. Nature 462, 863-867.

35. Laigle, M., Becel, A., de Voogd, B., Sachpazi, M., Bayrakci, G., Lebrun, J.-F., and Evain, M., 2013. Along-arc segmentation and interaction of subducting ridges with the Lesser Antilles subduction fore-arc crust revealed by MCS imaging. Tectonophysics, 603, 32-54.

36. Lajoie, K. R., 1986. Coastal Tectonics. Active tectonic. N. A. Press. Washington D, C, National Academic Press, 95-124.

37. Lallemand, S. E., 1995. High rates of arc consumption by subduction processes: some consequences. Geology, 23, 551-554.

721 38. Lallemand, S.E., 1999. La subduction océanique. Overseas Publishers Association, Gordon and
722 Breach Science Publishers, London, 194 p.
723
724 39. Lardeaux, J.-M., Münch, P., Corsini, M., Cornée, J.-J., Verati, C., Lebrun, J.-F., Quillévéré, F.,
725 Melinte-Dobrinescu, M., Léticée, J.-L., Fietzke, J., Mazabraud, Y., Cordey, F. and Randrianasolo,
726 A., 2013. La Désirade island (Guadeloupe, French West Indies): a key target for deciphering the
727 role of reactivated tectonic structures in Lesser Antilles arc building. Bulletin de La Société
728 Géologique de France, 184, 21-34.
729
730 40. Lasserre, G., 1961. La Guadeloupe: étude géographie (Vol. 2). Union française d'Impression, 2 vol
731 Bordeaux, France, gr.in-8*, 1135 pp.
732 https://www.abebooks.fr/servlet/BookDetailsPL?bi=5796175183&searchurl=tn%3Dla%2Bguadel
733 oupe%2Betude%2Bg%25E9ographique%26sortby%3D17%26an%3Dguy%2Blasserre
734
735 41. Laurencin, M., Marcaillou, B., Graindorge, D., Klingelhoefer, F., Lallemand, S., Laigle, M., &
736 Lebrun, J. F., 2017. The polyphased tectonic evolution of the Anegada Passage in the northern
737 Lesser Antilles subduction zone. *Tectonics*, *36*(5), 945-961.
738
739 42. Léticée, J. ‐ L., 2008. Architecture d'une plateforme carbonatée insulaire plio ‐ pleistocène en
740 domaine de marge active (avant ‐ arc des Petites Antilles, Guadeloupe): Chronostratigraphie,
741 sédimentologie paléoenvironnements. Unpublished PhD Thesis, Pointe à Pitre, Université des
742 Antilles et de la Guyane, 261 pp. http://www.diffusiontheses.fr/59450-these-de-leticee-jean-
743 len.html
744
745 43. Lisiecki, L. E. and Raymo, M. E., 2005. A Pliocene-Pleistocene stack of 57 globally distributed
746 benthic δ18O records. Paleoceanography, 20.1.: PA1003.

44. Mann, P., Taylor, F.W, Lawrence Edwards, R., and Teh-Lung Ku, 1995. Actively evolving microplate formation by oblique collision and sideways motion along strike-slip faults: An example from the northeastern Caribbean plate margin. Tectonophysics, 246, 1-69

45. McCann, W.R., and Sykes, L.R., 1984. Subduction of aseismic ridges beneath the Caribbean Plate: Implications for the tectonics and seismic potential of the northeastern Caribbean. Journal of Geophysical Research: Solid Earth, 89, 4493-4519.

46. Montaggioni, L. F. and Braithwaite, C. J., 2009. Quaternary Reefs in time and space. Developments in Marine Geology, 5, 1-21.

47. Münch, P., Lebrun, J. ‐ F., Cornée, J. ‐ J., Thinon, I., Guennoc, P., Marcaillou, B., Begot, J., Bertrand, G., Bes de Berc, S., Biscarrat, K., Claud, C., De Min, L., Fournier, F., Gailler, L. ‐ S., Graindorge, D., Léticée, J. ‐ L., Marié, L., Mazabraud, Y., Melinte Dobrinescu, M., Moissette, P., Quillévéré, F., Verati, C. and Randrianasolo, A., 2013. Pliocene to Pleistocene carbonate systems of the Guadeloupe archipelago, French Lesser Antilles: a land and sea study (the KaShallow project). Bulletin de la Société Géologique de France, 184, 99-110.

48. Münch, P., Cornée, J.-J., Lebrun, J.-F., Quillevere, F., Verati, C., Melinte-Dobrinescu, M., Demory, F., Smith, B., Jourdan, F., Lardeaux, J.-M., De Min, L., Leticée, J.-L. and Randrianasolo, A., 2014. Pliocene to Pleistocene vertical movements in the fore-arc of the Lesser Antilles subduction: insights from chronostratigraphy of shallow-water carbonate platforms (Guadeloupe archipelago). Journal of the Geological Society of London, 171, 329-341.

772 49. Murray-Wallace, C. and Woodroffe, C., 2014. Quaternary sea level: a global perspective.
773 Cambridge, Cambridge University Press.
774
775 50. Noda, A., 2016. Forearc basins: types, geometries, and relationships to subduction zone
776 dynamics. GSA Bulletin, 128, 879-895.
777
778 51. Patriat, M., Pichot, T., Westbrook, G.K., Umber, M., Deville, E., Benard, F., Roest, W.R., Loubrieu,
779 B. and Party, A.C., 2011. Evidence for Quaternary convergence across the North America-South
780 America plate boundary zone, east of the Lesser Antilles. Geology, 39, 979-982.
781
782 52. Pedoja, K., L. Husson, V. Regard, P. R. Cobbold, E. Ostanciaux, M. E. Johnson, S. Kershaw, M.
783 Saillard, J. Martinod, L. Furgerot, P. Weill and B. Delcaillau, 2011. Relative sea-level fall since the
784 last interglacial stage: Are coasts uplifting worldwide? Earth-Science Reviews 108, 1-15.
785
786 53. Pedoja, K., L. Husson, M. E. Johnson, D. Melnick, C. Witt, S. Pochat, M. Nexer, B. Delcaillau, T.
787 Pinegina, Y. Poprawski, C. Authemayou, M. Elliot, V. Regard and F. Garestier, 2014. Coastal
788 staircase sequences reflecting sea-level oscillations and tectonic uplift during the Quaternary and
789 Neogene. Earth-Science Reviews 132, 13-38.
790
791 54. Pichot, T., Patriat, M., Westbrook, G.K., Nalpas, T., Gutscher, M.A., Roest, W.R., Deville, E.,
792 Moulin, M., Aslanian, D. and Rabineau, M., 2012. The Cenozoic tectonostratigraphic evolution of
793 the Barracuda Ridge and Tiburon Rise, at the western end of the North America–South America
794 plate boundary zone. Marine Geology, 303–306, 154-171.
795
796 55. Pindell, J.L. and Kennan, L., 2009. Tectonic evolution of the Gulf of Mexico, Caribbean and
797 northern South America in the mantle reference frame: an update. In: James, K.H., Lorente, M.A.,

and Pindell, J.L., eds., Origin and Evolution of the Caribbean Plate. Geological Society, Special Publication, 328, 1-55.

56. Pirazzoli, P. A., U. Radtke, W. S. Hantoro, C. Jouannic, C. T. Hoang, C. Causse and Best M. B., 1993. A one million-year-long sequence of marine terraces on Sumba Island, Indonesia. Marine Geology 109, 221-236.

57. Rohling, E.J., Foster, G.L., Grant, K.M., Marino, G., Roberts, A.P., Tamisiea, M.E. and Williams, F., 2014. Sea-level and deep-sea-temperature variability over the past 5.3 million years. Nature, 508, 477-482.

58. Ruiz, M., Galve, A., Monfret, T., Sapin, M., Charvis, P., Laigle, M., Evain, M ., Hirn, A., Flueh, J., Diaz, J., Lebrun J.F, and the Lesser AntillesThales scientific party, 2013. Seismic activity offshore Martinique and Dominica islands (Central Lesser Antilles subduction zone) from temporary onshore and offshore seismic networks. Tectonophysics, 603, 68-78.

59. Saillard, M., Audin, L., Rousset, B., Avouac, J. P., Chlieh, M., Hall, S. R., Husson, L. and Farber, D. L., 2017. From the seismic cycle to long-term deformation: linking seismic coupling and Quaternary coastal geomorphology along the Andean megathrust. Tectonics, 36, 241-256.

60. Saillard, M., S. R. Hall, L. Audin, D. L. Farber, G. Hérail, J. Martinod, V. Regard, R. C. Finkel and Bondoux, F.,2009. Non-steady long-term uplift rates and Pleistocene marine terrace development along the Andean margin of Chile (31°S) inferred from 10Be dating. Earth and Planetary Science Letters 277, 50-63.

61. Schlaphorst, D., Kendall, J.-M., Collier, J.S., Verdon, J.P., Blundy, J., Baptie, B., Latchman, J.L., Massin, F. and Bouin, M.-P., 2016. Water, oceanic fracture zones and the lubrication of subducting plate boundaries—insights from seismicity. Geophysical Journal International, 204, 1405–1420.

62. Shemenda, A.I., 1994. Subduction. Insights from physical modeling. London, Kluwer Academic Publishers, 215 p.

63. Schellmann, G., and Radtke, U., 2004. A revised morpho-and chronostratigraphy of the Late and Middle Pleistocene coral reef terraces on Southern Barbados (West Indies). *Earth-Science Reviews,* 64, 157-187.

64. Sieh, K., Ward, S. N., Natawidjaja, D., & Suwargadi, B. W. (1999). Crustal deformation at the Sumatran subduction zone revealed by coral rings. Geophysical Research Letters, 26(20), 3141-3144.

65. Speed, R. C. and Cheng, H., 2004. Evolution of marine terraces and sea level in the last interglacial, Cave Hill, Barbados. Geological Society of America Bulletin 116, 219-232.

66. Taylor, F. W. and Mann, P. (1991). Late Quaternary folding of coral reef terraces, Barbados. *Geology*, 19, 103-106.

67. Tucker, M. E. and Wright, V. P., 1990. Diagenetic processes, products and environments. In: Carbonate sedimentology, Blackwell Publishing Ltd, Oxford, U.K., 314-364. doi: 10.1002/9781444314175.ch7

68. Vannucchi, P., Sak, P.B., Morgan, J.P., Ohkushi, K.i., Ujiie, K., Scientists, t.I.E.S., 2013. Rapid pulses of uplift, subsidence, and subduction erosion offshore Central America: implications for building the rock record of convergent margins. Geology 41, 995–998.

69. Veron, J. E. N., 2000. Corals of the World, vol. 1–3. Australian Institute of Marine Science, Townsville, 404-405.

70. Villemant, B. and Feuillet, N., 2003. Dating open systems by the 238 U–234 U–230 Th method: application to Quaternary reef terraces. Earth and Planetary Science Letters, 210, 105-118.

71. von Huene, R., Culotta, R., 1989. Tectonic erosion at the front of the Japan Trench convergent margin. Tectonophysics 160, 75–90.

72. von Huene, R. and Ranero, C.R., 2003. Subduction erosion and basal friction along the sediment-starved convergent margin off Antofagasta, Chile. Journal of Geophysical Research: Solid Earth, 108.B2.

73. Von Huene, R., Miller, J. J., and Weinrebe, W.,2012. Subducting plate geology in three great earthquake ruptures of the western Alaska margin, Kodiak to Unimak. Geosphere,8 , 628-644.

74. Westercamp, D., 1980. La Désirade, carte géologique à 1: 25 000 et notice explicative. Service Géologique National, Bureau de Recherches Geologiques et Minières, Orléans, France.

Figures caption

Fig. 1. Location of the studied area in the Lesser Antilles subduction zone (from Feuillet et al., 2002 and Münch et al., 2014).

Fig. 2. Main geological features of the Guadeloupe Archipelago, from Léticée (2008), Münch et al. (2014) and De Min (2014). 1 to 7: dated Pleistocene terraces: 1, Anse Laborde (Battistini et al., 1986); 2, Pointe Noire (Feuillet et al., 2004); 3, Anse à l'Eau (this work) ; 4, Pointe Tarare (Feuillet et al., 2004); 5, SW Désirade (Battistini et al., 1986; Feuillet et al., 2004); 6, Baie Mahault (Battistini et al., 1986) ; 7, Marie Galante (Battistini et al., 1986; Feuillet et al., 2004).

Fig. 3. A: Geological map of La Désirade, from Westercamp (1980), modified from new field investigations (this study); B: Lithostratigraphic succession, referred to the Grande Terre succession (Cornée et al., 2012; Münch et al., 2014); C: Cross section displaying the Present-day elevations of the investigated coral reef deposits.

Fig. 4. The Upper Plateaus. A: general view of the southern coast towards SW from Baie Mahault area; B: general view of Pointe Adrien, northern coast; C: partially dissolved *Acropora palmata* coral colonies (arrows; northeastern part of the Upper Plateaus).

Fig. 5. A: DNM with the marine terraces in the northeastern part of La Désirade; B: DNM with marine terraces in southern part of La Désirade; C: topographic profiles with location of the paleoshorelines surfaces; D: terminology of the different elements for the description of the terraces.

898

899 Fig. 6. Terrace 1 (loc. Fig. 3). A: field view of the 90 m asl and 76 m asl terraces surface in the Pointe
900 du Grand Abaque area; B: conglomeratic limestone with sandy calcareous matrix, red algae and
901 benthic foraminifers; pebbles are encrusted by red algae (arrows).

902

903 Fig. 7. Terrace 2 (loc. Fig. 3). A: field view of the +76 m terrace surface (arrows), Baie mahault area
904 (southern side of La Désirade); B: succession of terrace 2 at Route de La Montagne; C: field view of
905 the succession; D: cross stratification (upper arrow) and hummocky cross stratification (lower arrow)
906 in matrix supported conglomerates and microconglomeratic sandstones; E: aragonite *Diploria* coral
907 colony; F: and G microscopic views of the aragonite walls of the corals (natural light).

908

909 Fig. 8. Terrace 3 (loc. Fig. 3). A: Terraces 3 and 4 at Cul Foncé; B: lithological succession in the terrace
910 3 at Cul Foncé; C: terrace 3 at Pointe Doublé; D: horizontal wavecut surface at + 36 m, Roche du
911 large. Same legend as Fig. 7.

912

913 Fig. 9. Marine deposits of Terrace 3, Cul Foncé (loc. Fig. 3). A: conglomerates with pebbles above the
914 basement; B: 3D dunes in vertical accretion; C: parallel-bedding laminations with pebbly intervals
915 (center) and cross-trough stratification (lower arrow); D: cross-stratification; E: aragonite massive
916 coral colony DS 10-40; F: microscopic view of the coral colony (natural light). Same legend as Fig. 7.

917

918 Fig. 10. Terrace 4, Pointe Frégule (loc. Fig. 3). A: lithostratigraphic succession; B: low angle planar
919 lamination; C: basal conglomerate; D: large *Acropora palmata* colonies (arrows); E: microscopic view
920 of aragonite walls of the coral colonies (natural light). Hammer is 40 cm long. Same legend as Fig. 7.

Fig. 11. Terrace 4, Pointe Fromager, northern coast of La Désirade (loc. Fig. 3).

Fig. 12. Terrace 4 (loc. Fig. 3). A: field view at Baie Mahault beach (near cemetery); B: Dated coral at Baie Mahault beach; C: microscopic view of the aragonite corals DS11-43 at Baie Mahault beach; D: *Acropora palmata* boudstone (arrows); E: massive *Montastraea* colony (hammer is cm long); F: terraces 3 and 4 at Pointe Mancenillier (loc. Fig. 3).

Fig. 13. Morphostratigraphy and apparent uplift rates at La Désirade. Marine isotopic stages from Lisiecki and Raymo (2005) and sea level estimates from Rohling et al. (2014).

Fig. 14. Ages and elevations of the marine terraces in the Guadeloupean archipelago. Guadeloupe: Battistini et al. (1986); Münch et al. (2013; 2014); Marie Galante: Feuillet et al. (2004); La Désirade: this work.

Fig. 15. A: Calabrian uplifts at La Désirade; B: distribution of vertical motions and location of the Tiburon Ridge below the Karukéra Spur in the Guadeloupe archipelago during Calabrian; C: Ionian to Recent uplift at La Désirade; D: distribution of vertical motions and location of the Tiburon Ridge below the Karukéra Spur in the Guadeloupe archipelago during Ionian to Recent. Reconstructions are based on Andreïeff et al., (1989), Bouysse and Westercamp (1990), Gailler et al. (2013), De Min (2014) and De Min et al. (2015).

Table caption

Table 1. Blank amounts of the isotopes used for U/Th dating.

Table 2. U-series results of La Désirade and Grande Terre fossil coral samples (all uncertainties quoted at 95% confidence level). For the correction of detrital ^{230}Th a ^{230}Th/^{232}Th activity ratio of 0.6 ± 0.2 has been applied.

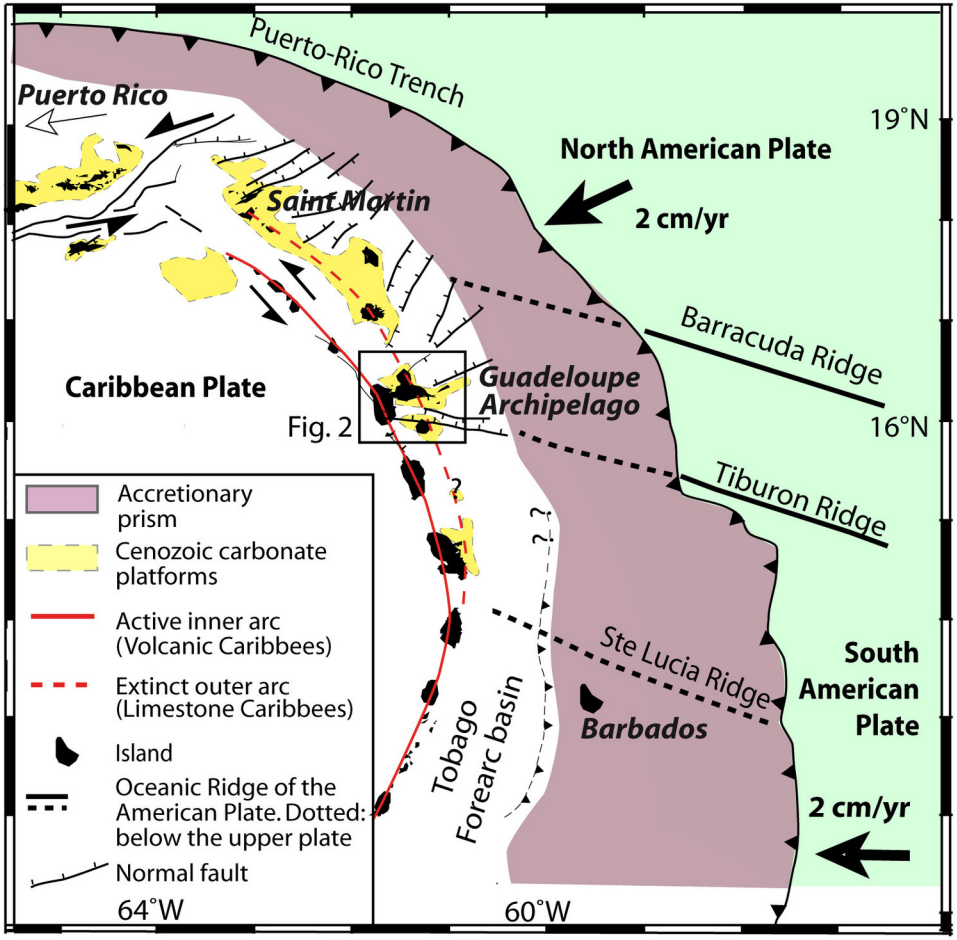

Fig. 1. Léticée et al.

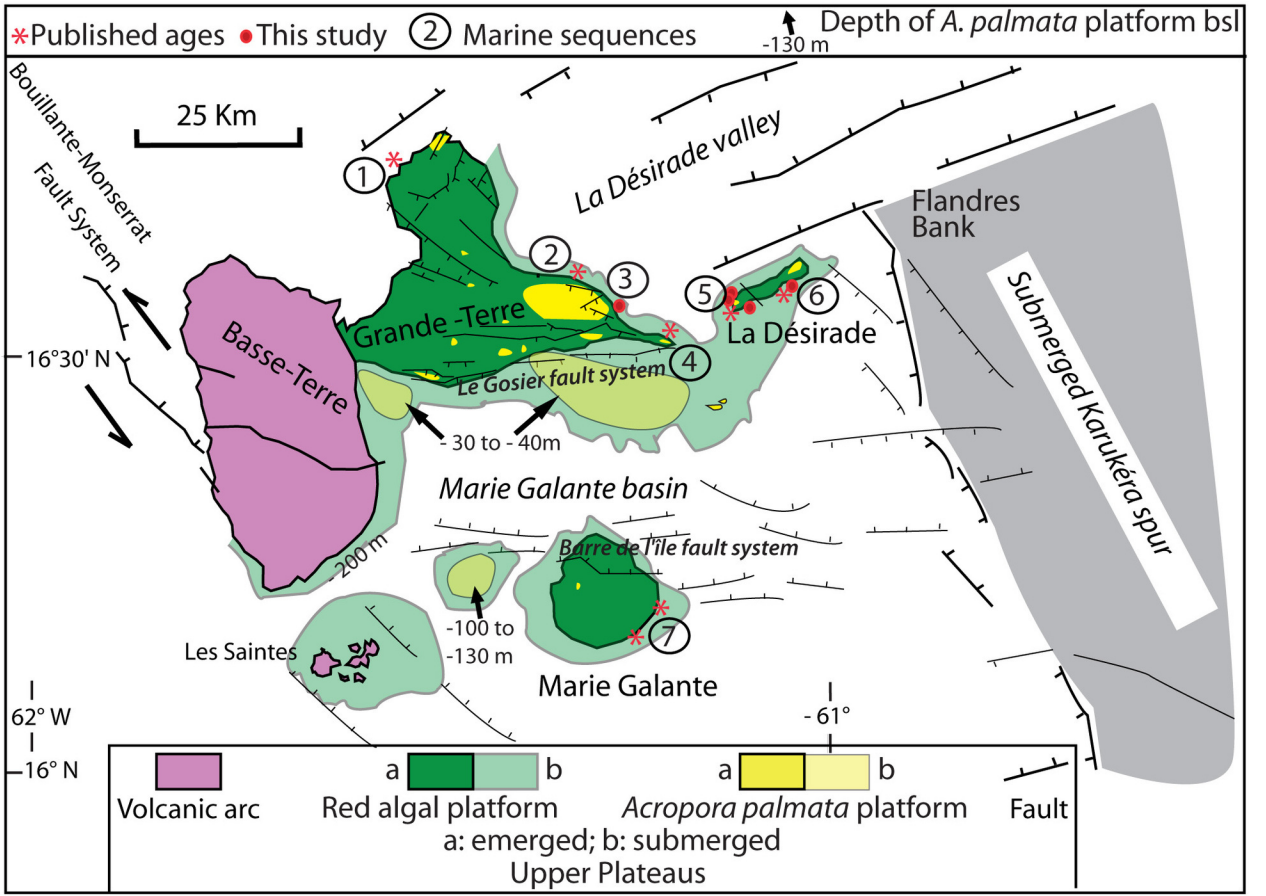

Léticée et al., Fig. 2

Léticée et al., Fig.3.

METTRE AUTRES FIGS

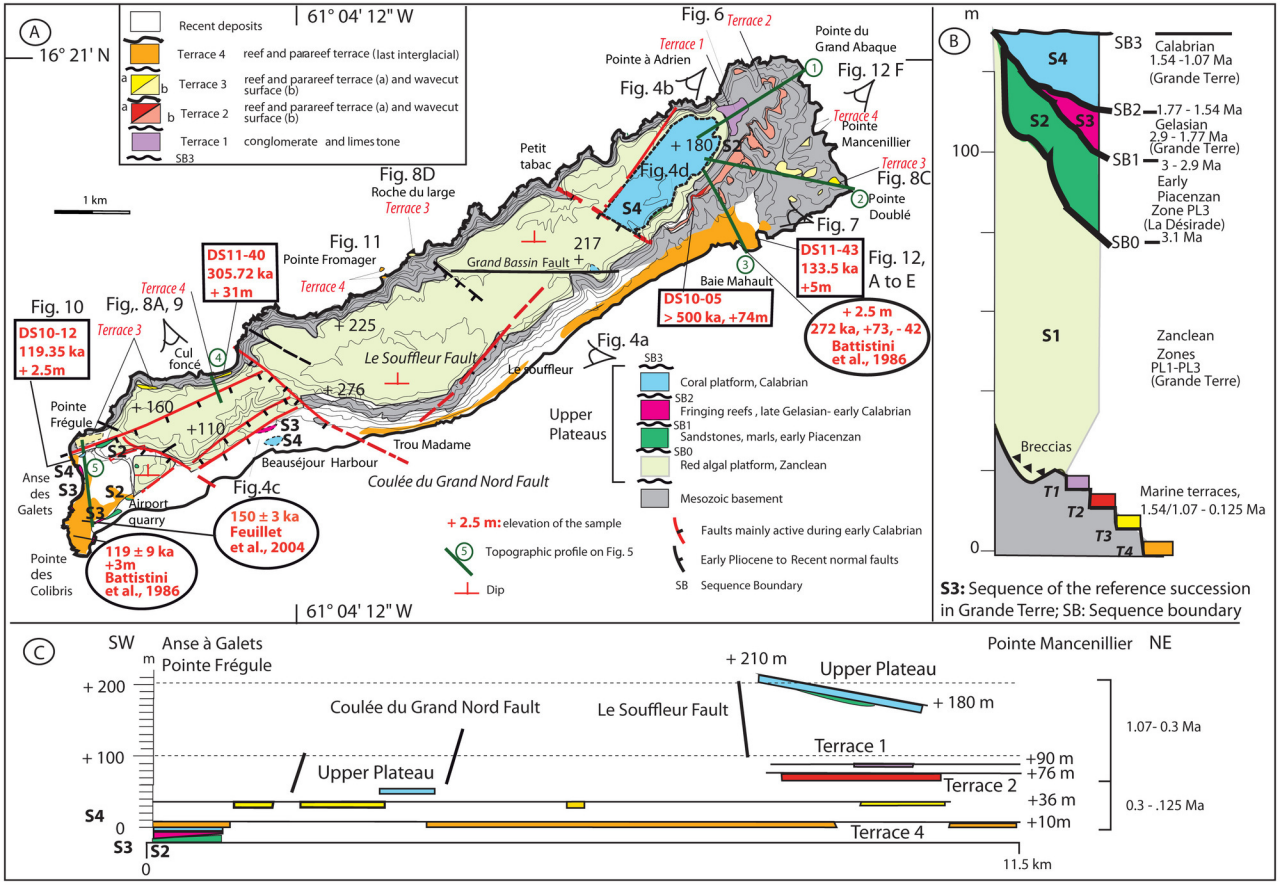

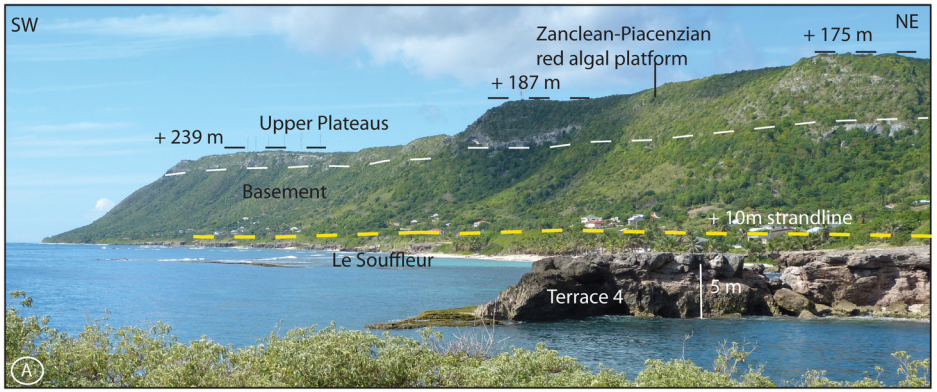

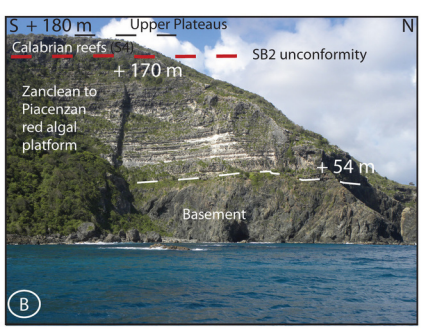

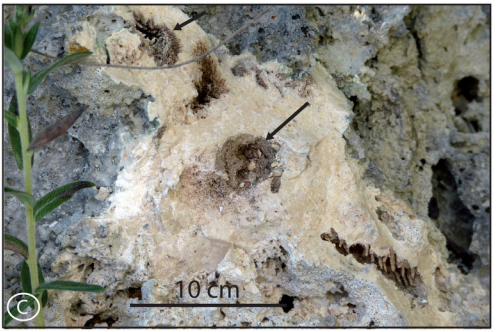

Léticée et al., Fig. 4

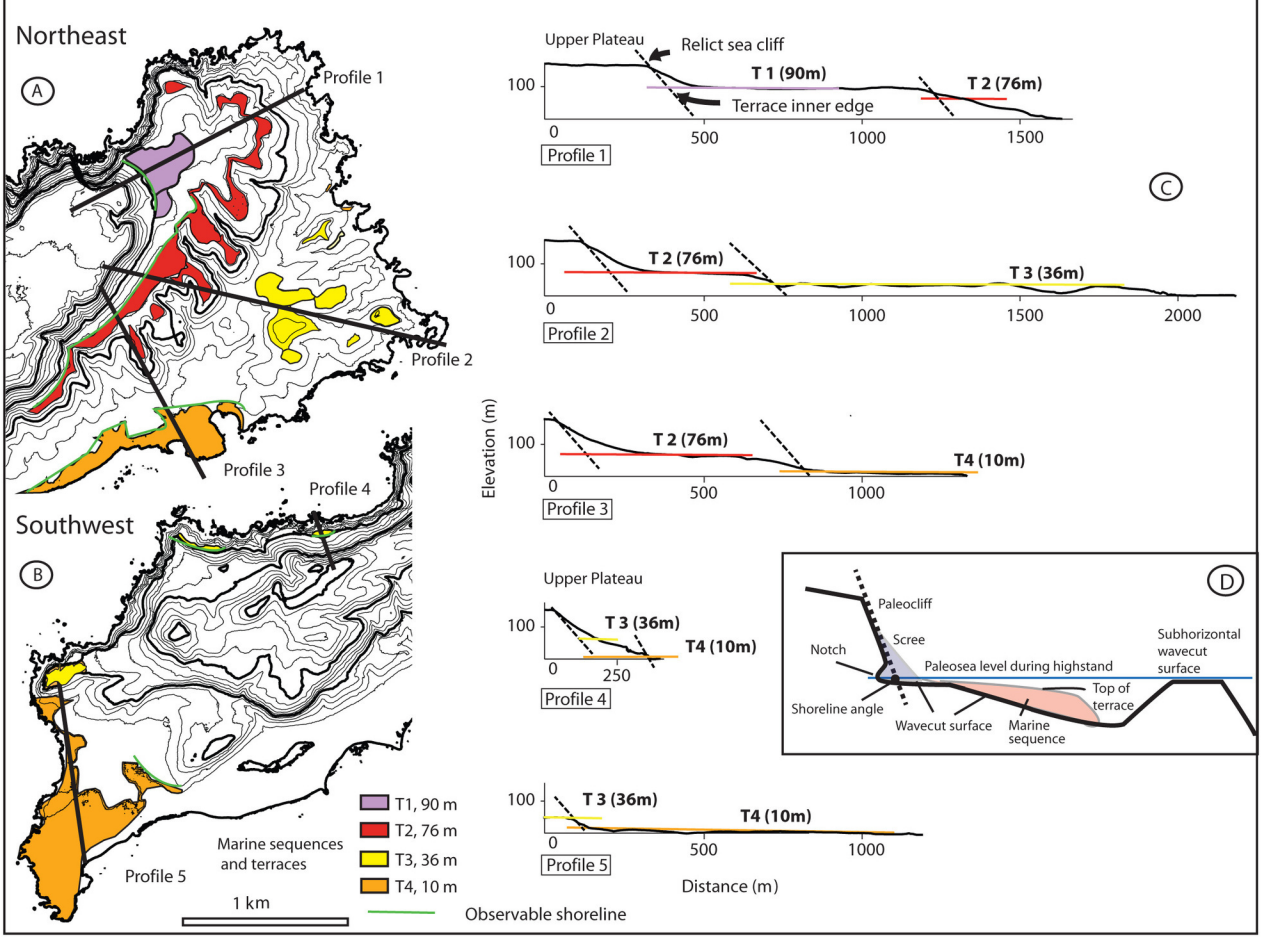

Leticee et al., fig. 5

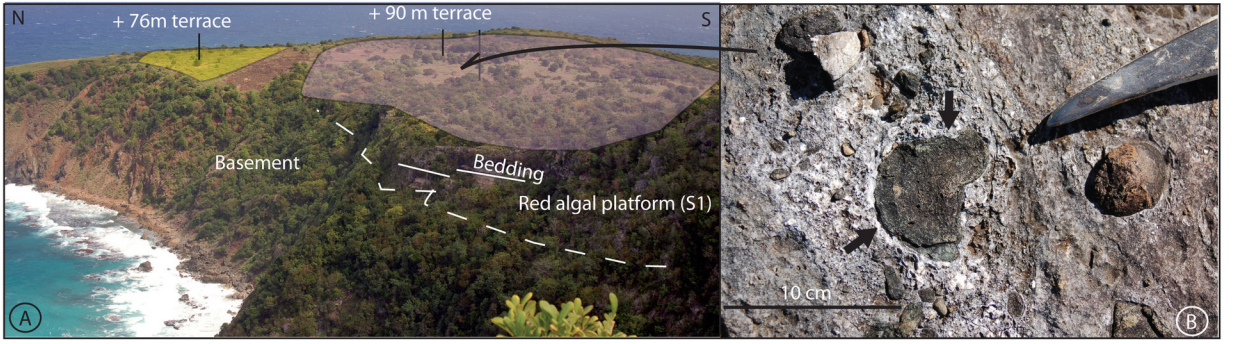

Léticée et al., fig. 6

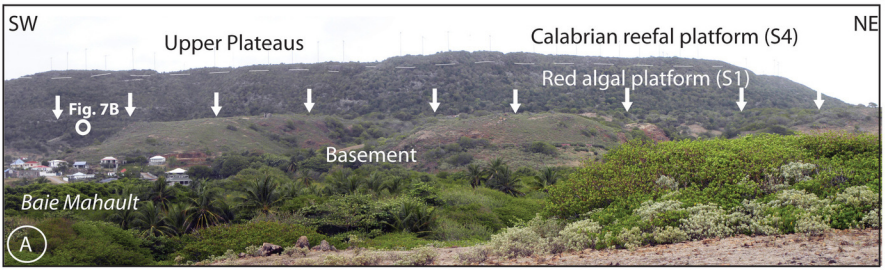

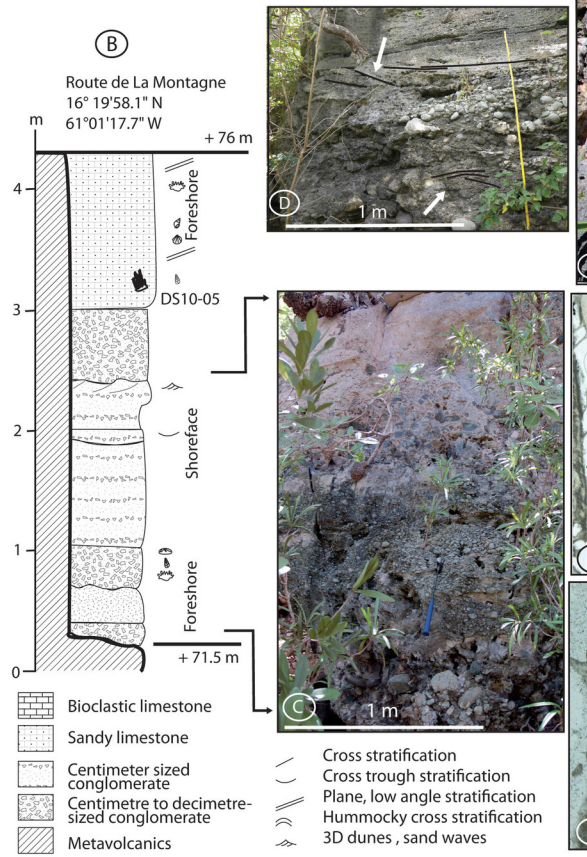

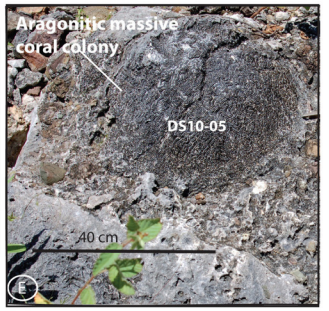

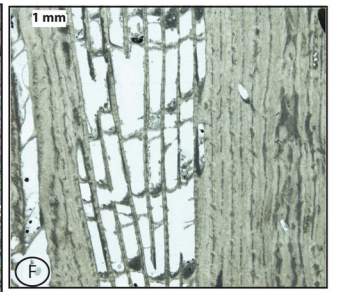

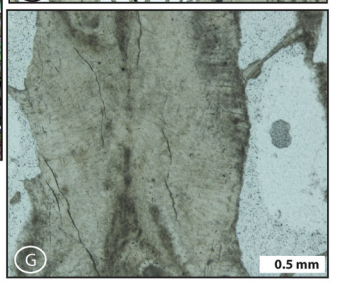

Léticée et al., Fig. 7

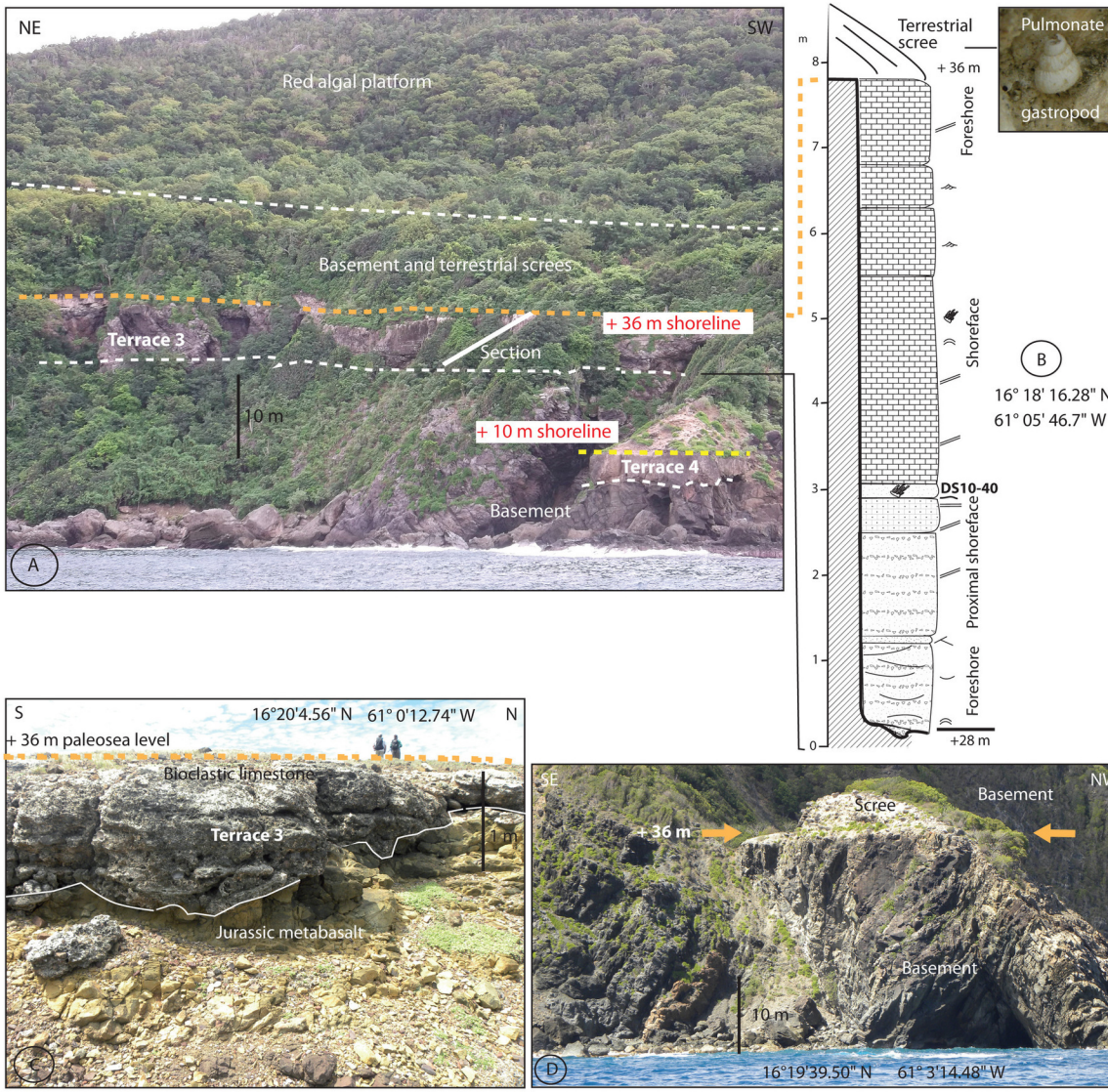

Léticée et al., Fig 8

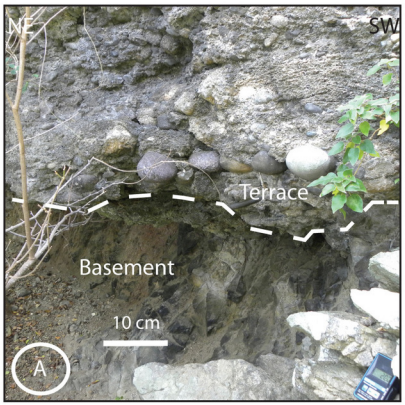

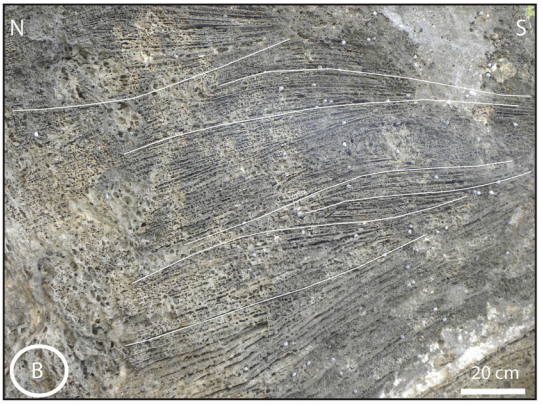

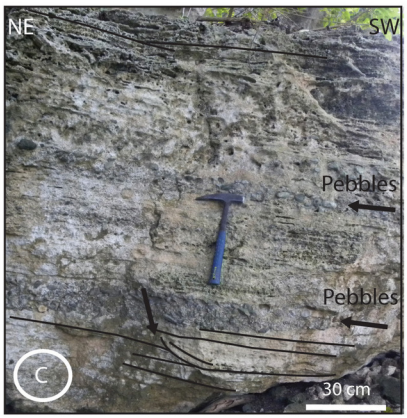

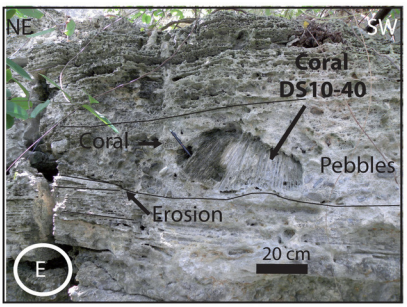

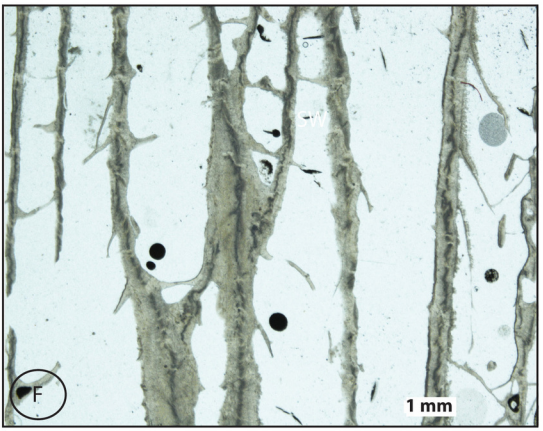

Léticee et al., Fig. 9

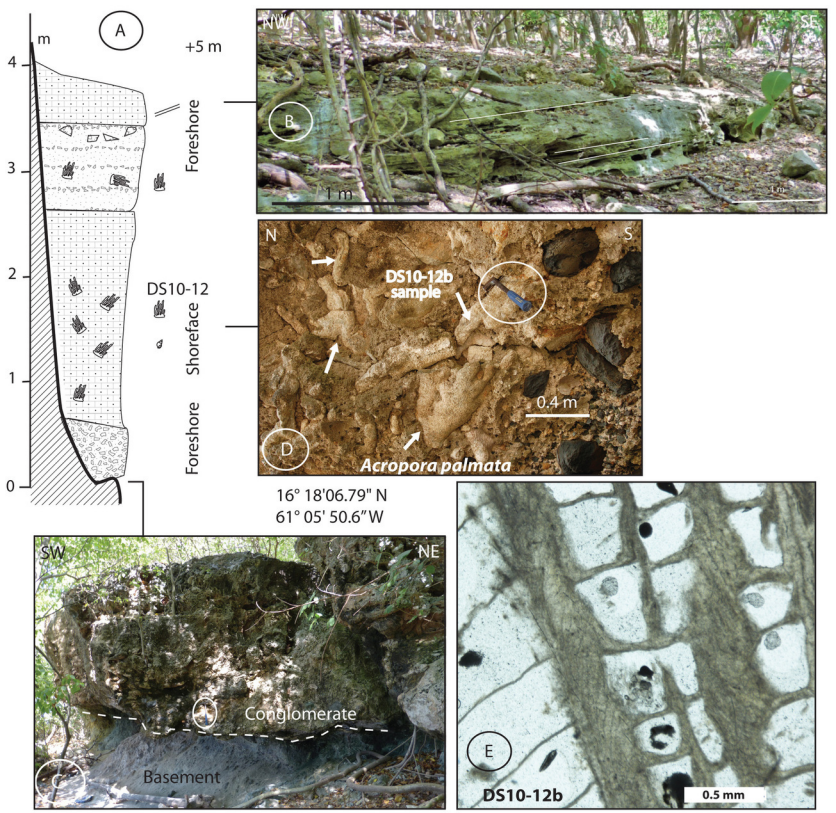

Léticée et al Fig. 10

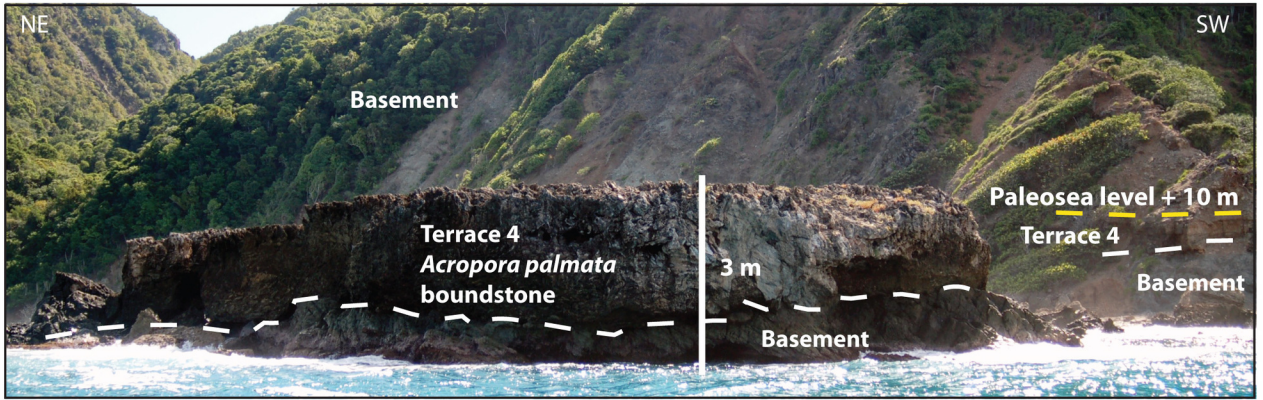

Léticée et al., fig. 11

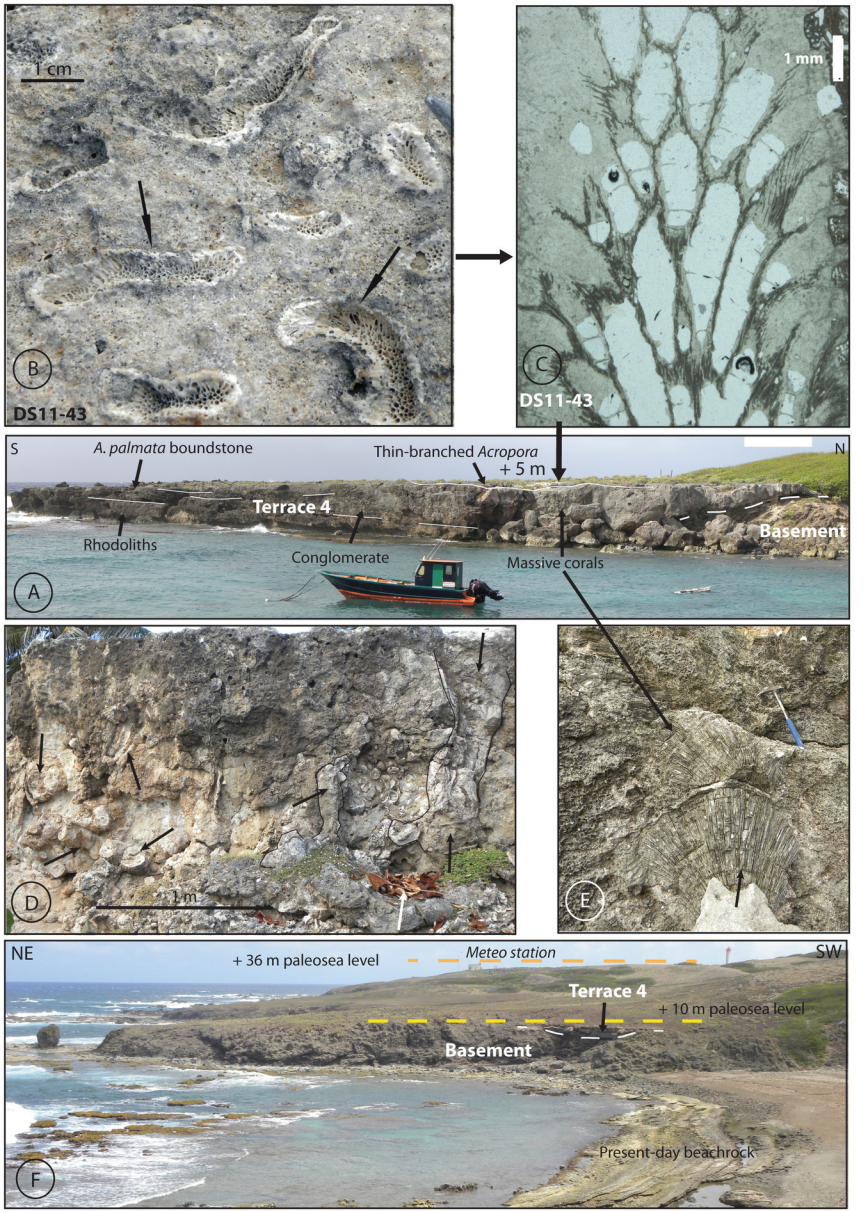

Léticée et al Fig. 12

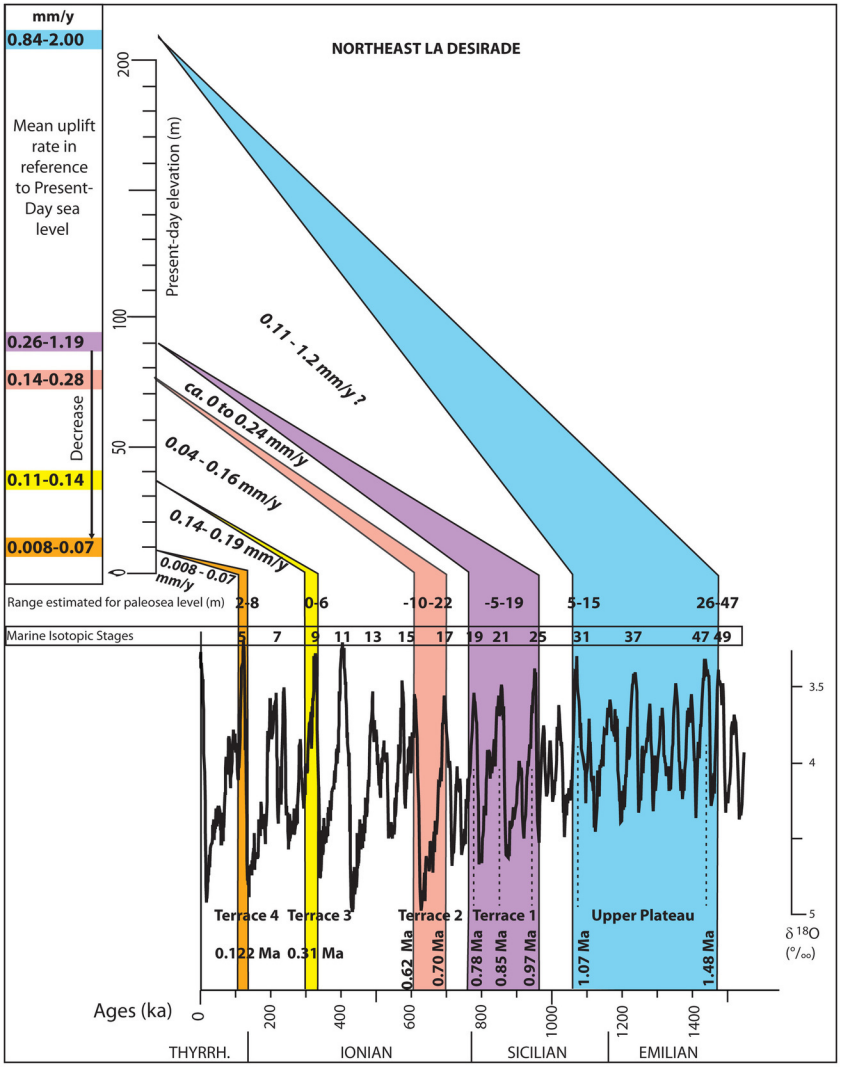
mm/y
0.84-2.00
Mean uplift rate in reference to Present-Day sea level
0.26-1.19
0.14-0.28
Decrease
0.11-0.14
0.008-0.07
NORTHEAST LA DESIRADE
Present-day elevation (m)
200
100
50
0
0.11 - 1.2 mm/y ?
ca. 0 to 0.24 mm/y
0.04 - 0.16 mm/y
0.14 - 0.19 mm/y
0.008 - 0.07 mm/y
Range estimated for paleosea level (m)
2-8
0-6
-10-22
-5-19
5-15
26-47
Marine Isotopic Stages
5 7 9 11 13 15 17 19 21 25 31 37 47 49
Terrace 4
0.122 Ma
Terrace 3
0.31 Ma
Terrace 2
0.62 Ma
0.70 Ma
Terrace 1
0.78 Ma
0.85 Ma
0.97 Ma
Upper Plateau
1.07 Ma
1.48 Ma
3.5
4
5
δ 18O (‰)
Ages (ka)
0
200
400
600
800
1000
1200
1400
THYRRH.
IONIAN
SICILIAN
EMILIAN

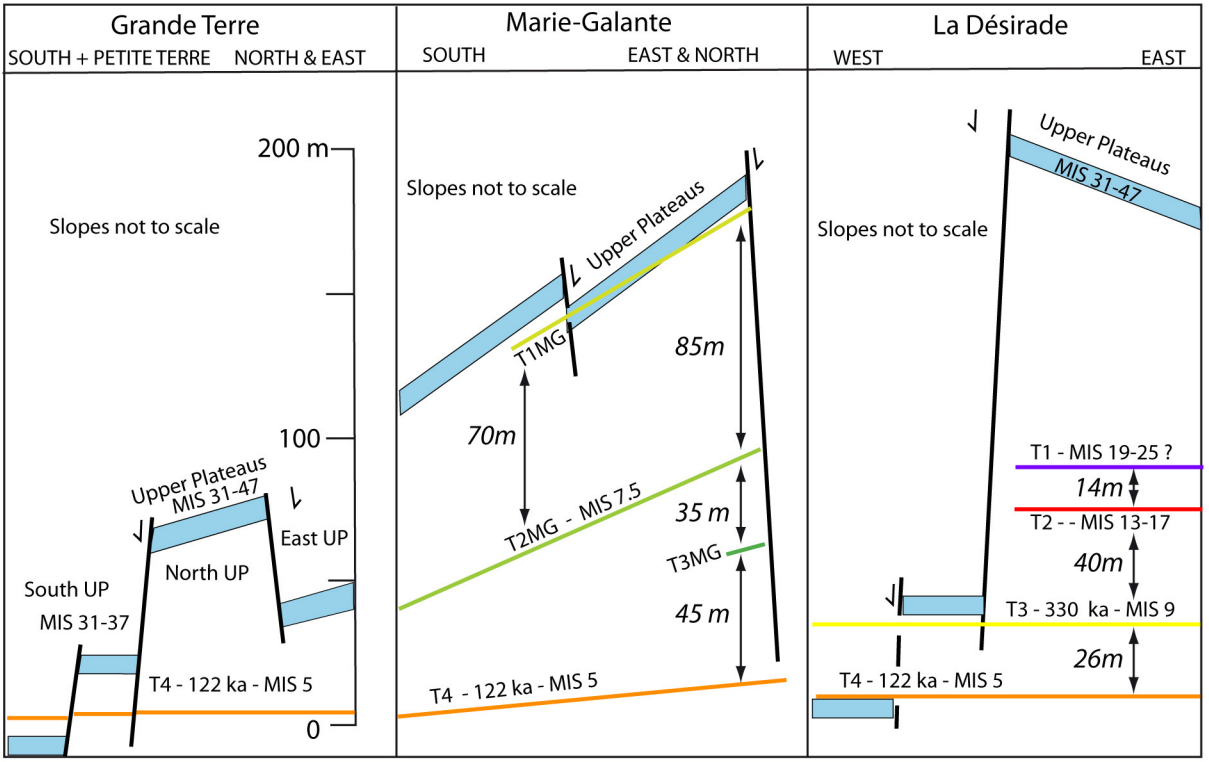

Léticée et al., fig. 14

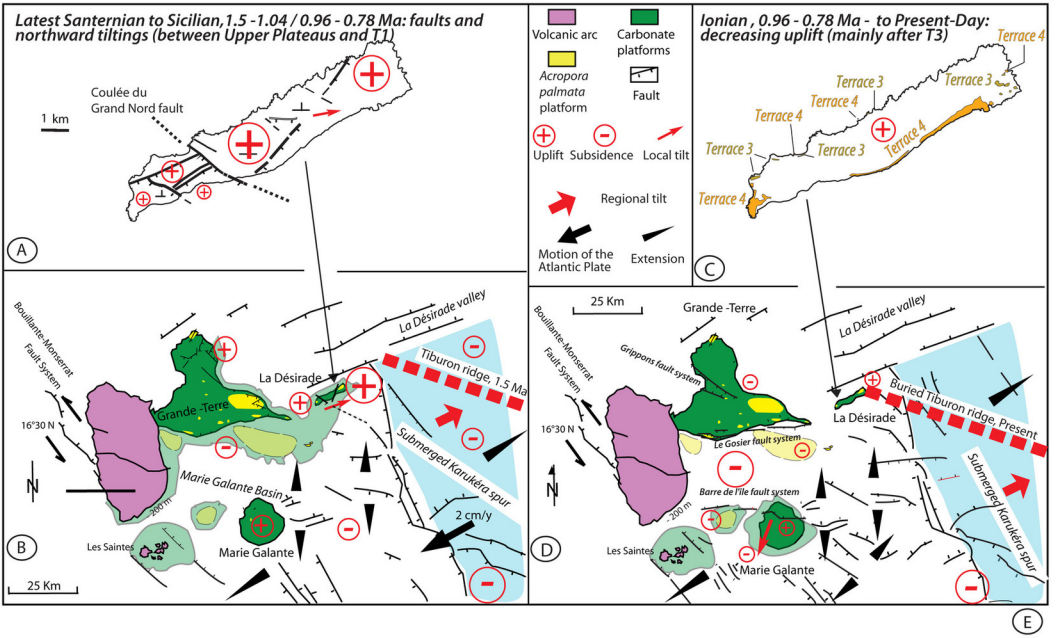

Léticée et al., Fig. 15

Léticée et al., Table 1

isotope	**blank in *g***
^{230}Th	(1.1 ± 0.6) e-16
^{232}Th	(4.2 ± 2.1) e-13
^{234}U	(7 ± 4) e-16
^{238}U	(9 ± 5) e-12

.

Sample	Age [ka]	^{238}U [ppm]	^{232}Th [ppb]	$^{230}Th/^{238}U$ [dpm/dpm]	$^{234}U/^{238}U$ [dpm/dpm]	$^{230}Th/^{232}Th$ [dpm/dpm]	Location of samples	Mineralogy
La Désirade								
DS 10-12a	126.09 ± 0.58	2.3507 ± 0.0014	0.7963 ± 0.0038	0.77708 ± 0.00085	1.1159 ± 0.0010	7100.7 ± 34.7	Terrace 4, Pointe Frégule, +2.5 m,	Aragonite 97%, Mg calcite 3%
DS 10-12b	128.19 ± 0.61	2.3035 ± 0.0013	1.0197 ± 0.0039	0.78772 ± 0.00106	1.1204 ± 0.0010	5508.2 ± 22.1	Terrace 4 Pointe Frégule, +2.5 m	Aragonite 97%, Mg calcite 3%
DS 11-43	133.50 ± 0.84	2.1278 ± 0.0018	1.6745 ± 0.0037	0.79796 ± 0.00100	1.1118 ± 0.0014	3138.6 ± 7.6	Terrace 4 Baie Mahault, + 5 m	Aragonite 96%, Calcite 4%
DS 11-40	305.72 ± 5.96	2.0724 ± 0.0015	0.6219 ± 0.0039	1.03372 ± 0.00162	1.0763 ± 0.0014	10661.8 ± 67.7	Terrace 3 Cul Foncé, + 31 m	Aragonite 97%, Mg calcite 3%
DS 10-05	>500	2.0977 ± 0.0010	0.6625 ± 0.0035	1.04099 ± 0.00125	1.0221 ± 0.0007	10202.9 ± 55.8	Terrace 2, route de La Montagne, + 74 m	Aragonite 96%, Mg calcite 4%
Grande Terre								
A-EAU 5	125.01 ± 0.44	2.3303 ± 0.0010	1.7116 ± 0.0036	0.77213 ± 0.00073	1.1141 ± 0.0007	3254.0 ± 7.3	Terrace 4 Anse à l'Eau, +5 m	Aragonite 97%, Mg calcite 3%

Léticée et al., Table 2